An Examination of C−H Bond Activation by Cationic $Tp^{Me_2}Ir(III)$ Complexes

David M. Tellers and Robert G. Bergman*

Department of Chemistry and Center for New Directions in Organic Synthesis, University of California, Berkeley, and Lawrence Berkeley National Laboratory, Berkeley, California 94720

Received August 1, 2001

Synthesis and characterization of a set of iridium(III) compounds utilizing the sterically encumbering hydridotris(3,5-dimethylpyrazolyl)borate ligand (Tp^{Me_2}) has been performed, and a comparison with the corresponding Cp* complexes is presented. $Tp^{Me_2}(PMe_3)Ir(Me)$-OTf (**7**, OTf = O_3SCF_3) was synthesized and found to be unreactive toward a variety of C−H bonds, in contrast to the behavior of $Cp^*(PMe_3)Ir(Me)OTf$ (**1**). We have rationalized this lack of reactivity in terms of an electronic effect rather than a steric effect imposed by the Tp^{Me_2} ligand. Metathesis of the triflate ligand with the BAr_f (BAr_f = B[3,5-$C_6H_3(CF_3)_2]_4$) anion under a N_2 atmosphere produces the dinitrogen complex $[Tp^{Me_2}(PMe_3)Ir(N_2)(Me)][BAr_f]$ (**3-N$_2$**). Compound **3-N$_2$** is indeed reactive toward dative ligands, H_2, and hydrocarbons, activating the C−H bonds of benzene and aldehydes but not those of saturated hydrocarbons. A rationale for the difference in behavior between the Cp* and Tp^{Me_2} systems with respect to C−H activation is presented.

Introduction

The controlled, efficient functionalization of saturated hydrocarbons remains an elusive goal.[1−5] We and others have focused on developing homogeneous transition metal complexes capable of catalytically dehydrogenating alkanes (eq 1).[6−10]

$$R{-}CH_2CH_3 \xrightarrow[[M]]{} R{-}CH{=}CH_2 + H_2 \qquad (1)$$

A general mechanism for the metal-catalyzed dehydrogenation of an alkane involves oxidative addition of the alkane to an unsaturated metal hydride species, reductive elimination of H_2, β-hydride elimination, and dissociation of the olefin to regenerate the metal hydride.[11] In addition to being able to activate the strong alkane C−H bond, the metal complex must neither bind the olefin product irreversibly[11] nor react with itself.

We previously reported the synthesis and study of two Ir(III) compounds, $Cp^*(PMe_3)Ir(Me)OTf$ (**1**) (Cp^* = C_5Me_5, OTf = OSO_2CF_3) and $[Cp^*(PMe_3)Ir(Me)(ClCH_2Cl)][BAr_f]$ (**2-CH_2Cl_2**) (BAr_f = B[3,5-$C_6H_3(CF_3)_2]_4$), that are capable of selectively cleaving carbon−hydrogen bonds in a wide variety of hydrocarbons under mild conditions (three examples are illustrated in Scheme 1).[12−17] The reaction of **1** or **2-CH_2Cl_2** with ethane, shown in Scheme 1, to produce the ethylene hydride complex $[Cp^*(PMe_3)IrH(CH_2CH_2)][X]$ (X = OTf, BAr_f) demonstrated that "$Cp^*(PMe_3)IrMe^+$" could potentially serve as a precursor to a dehydrogenation catalyst. Unfortunately, attempts to induce olefin dissociation from $[Cp^*(PMe_3)IrH(CH_2CH_2)][X]$ were unsuccessful. Additionally, the potential dehydrogenation catalyst, $[Cp^*(PMe_3)IrH(CH_2Cl_2)][X]$, irreversibly dimerizes at temperatures greater than −20 °C.[18]

Scheme 1

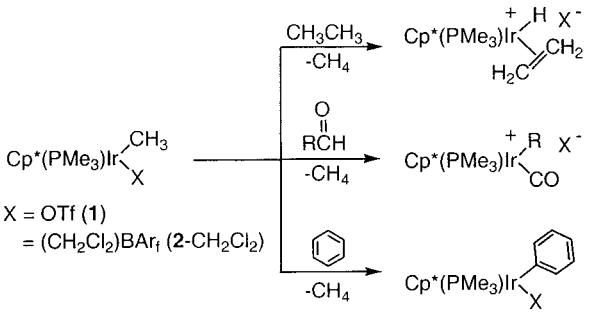

In an effort to address these shortcomings, we focused on increasing the size of the ancillary ligand at the metal center in hopes that this would lower the barrier of olefin dissociation from iridium and prevent the decomposition of an iridium hydride intermediate. One such ligand that would allow us to test this hypothesis

(1) Stahl, S. S.; Labinger, J. A.; Bercaw, J. E. *Angew. Chem., Int. Ed.* **1998**, *37*, 2181−2192.
(2) Sen, A. *Acc. Chem. Res.* **1998**, *31*, 550−557.
(3) Shilov, A. E.; Shul'pin, G. B. *Chem. Rev.* **1997**, *97*, 2879−2932.
(4) Arndtsen, B. A.; Bergman, R. G.; Mobley, T. A.; Peterson, T. H. *Acc. Chem. Res.* **1995**, *28*, 154−162.
(5) McCosh, D. *Pop. Sci.* **1999**, *254*, 56−59.
(6) For examples, see refs 7−10.
(7) Kanzelberger, M.; Singh, B.; Czerw, M.; Krogh-Jespersen, K.; Goldman, A. S. *J. Am. Chem. Soc.* **2000**, *122*, 11017−11018.
(8) Fuchen, L.; Pak, E. B.; Singh, B.; Jensen, C. M.; Goldman, A. S. *J. Am. Chem. Soc.* **1999**, *121*, 4086−4087.
(9) Gupta, M.; Hagen, C.; Kaska, W. C.; Cramer, R. E.; Jensen, C. M. *J. Am. Chem. Soc.* **1997**, *119*, 840−841.
(10) Aoki, T.; Crabtree, R. H. *Organometallics* **1993**, *12*, 294−298.
(11) Niu, S.; Hall, M. B. *J. Am. Chem. Soc.* **1999**, *121*, 3992−3999.
(12) Burger, P.; Bergman, R. G. *J. Am. Chem. Soc.* **1993**, *115*, 10462−10463.
(13) Arndtsen, B. A.; Bergman, R. G. *Science* **1995**, *270*, 1970−1973.
(14) Arndtsen, B. A.; Bergman, R. G. *J. Organomet. Chem.* **1995**, *504*, 143−146.
(15) Luecke, H. F.; Arndtsen, B. A.; Burger, P.; Bergman, R. G. *J. Am. Chem. Soc.* **1996**, *118*, 2517−2518.
(16) Alaimo, P. J.; Arndtsen, B. A.; Bergman, R. G. *Organometallics* **2000**, *19*, 2130−2143.
(17) Tellers, D. M.; Yung, C. M.; Arndtsen, B. A.; Bergman, R. G. Submitted for publication.
(18) Golden, J. T.; Andersen, R. A.; Bergman, R. G. *J. Am. Chem. Soc.* **2001**, *123*, 5837−5838.

10.1021/om010697c CCC: $20.00
Publication on Web 10/10/2001

Scheme 2

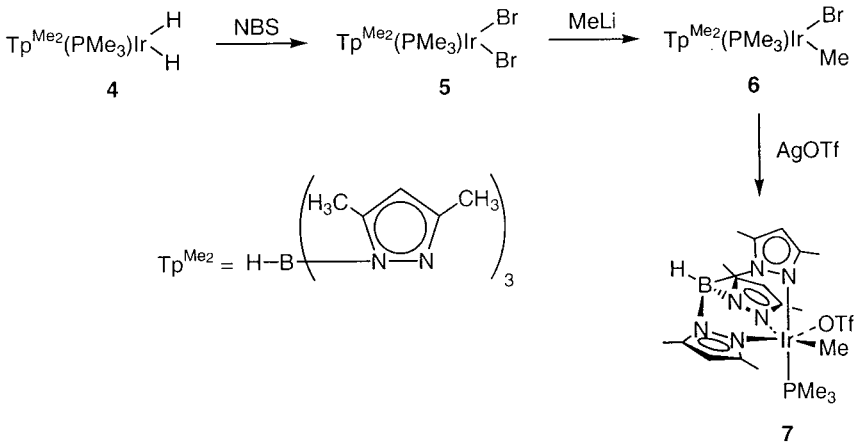

is the hydridotris(3,5-dimethylpyrazolyl)borate (Tp^{Me_2}) ligand. The Tp^{Me_2} ligand is isoelectronic to Cp* but occupies substantially increased space in the coordination sphere of metals.[19,20] We therefore decided to develop the methodology needed to synthesize the Tp^{Me_2} analogues of **1** and **2** and investigate their C−H activating properties, hoping that the use of the bulky Tp^{Me_2} ligand would promote rapid formation of the corresponding 16-electron Ir cations.[21]

This paper details the preparation of a series of Tp^{Me_2}-Ir(III) compounds, including $Tp^{Me_2}(PMe_3)Ir(Me)OTf$ (**7**).[22] This compound does not react with C−H bonds, and an examination of the differences between the Tp^{Me_2} and Cp* ligands revealed that this lack of reactivity is the result of an electronic effect imposed by the Tp^{Me_2} ligand. Salt metathesis with **7** facilitated the synthesis of $[Tp^{Me_2}(PMe_3)Ir(Me)N_2][BAr_f]$ (**3-N₂**), the first structurally characterized monomeric iridium dinitrogen complex. The reactions of **3-N₂** with dative ligands, C−H bonds, and H_2 are detailed herein.

Results

Synthesis of the Tp^{Me_2}Ir(III) Complexes. Routes analogous to those used in the synthesis of compounds **1**[12] and **2**[13] were not successful with the Tp^{Me_2} ligand. As a result, we developed a new route into the $Tp^{Me_2}(PMe_3)IrMe(X)$ systems (Scheme 2). Treatment of $Tp^{Me_2}(PMe_3)IrH_2$ (**4**)[23] with 2 equiv of NBS in CCl_4 resulted in the clean formation of $Tp^{Me_2}(PMe_3)IrBr_2$ (**5**) (53% yield). This compound can be selectively monoalkylated with methyllithium to generate $Tp^{Me_2}(PMe_3)Ir(Me)Br$ (**6**) (62% yield), which underwent facile anion metathesis upon treatment with AgOTf to provide $Tp^{Me_2}(PMe_3)Ir(Me)OTf$ (**7**) (47% yield). The structure of **7** was determined by X-ray crystallography (Figure 1). Interestingly, the Ir−O bond length of 2.128(5) Å in **7** is much shorter than the analogous bond length in $Cp^*(PMe_3)Ir(Me)OTf$ (**1**) (2.216(10) Å).[12] The data collection and refinement parameters are listed in Table 5, and a list of selected bond distances and angles is located in Table 1.

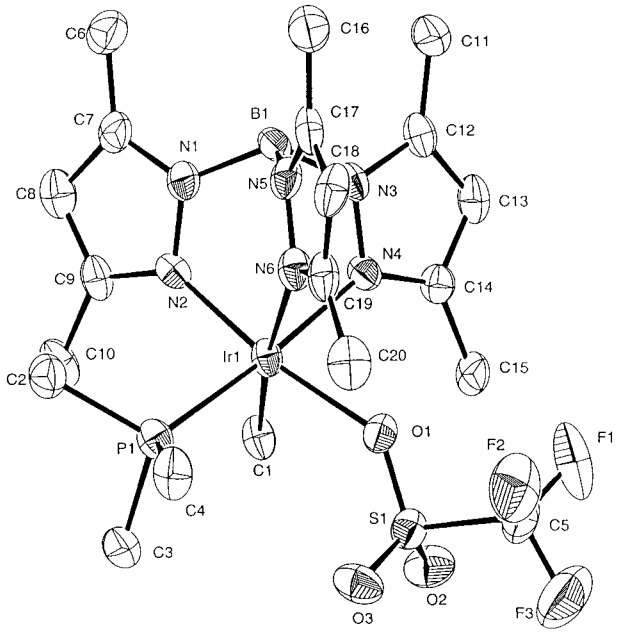

Figure 1. ORTEP diagram of $Tp^{Me_2}(PMe_3)IrMeOTf$ (**7**). Thermal ellipsoids are shown at the 50% probability level. Hydrogen atoms are omitted for clarity.

Table 1. Selected Intramolecular Distances and Angles for $Tp^{Me_2}(PMe_3)IrMeOTf$ (7)

	Distance (Å)		
Ir−O(1)	2.128(5)	Ir−N(2)	2.028(6)
Ir−C(1)	2.098(7)	Ir−N(4)	2.134(6)
Ir−P(1)	2.289(2)	Ir −N(6)	2.230(6)
	Angles (deg)		
O(1)−Ir(1)−C(1)	91.2(2)	N(2)−Ir(1)−N(4)	84.7(2)
C(1)−Ir(1)−P(1)	92.6(2)	N(4)−Ir(1)−N(6)	84.0(2)
P(1)−Ir(1)−O(1)	97.5(1)	N(6)−Ir(1)−N(2)	94.3(2)

This short Ir−O bond length presaged our finding that triflate **7** is unreactive toward a variety of hydrocarbons, including benzene and methane. This stands in contrast to the behavior of the Cp* analogue **1**, which rapidly cleaves the C−H bonds of all these substrates.[12] Complex **7** is also inert toward Lewis bases. Displacement of the triflate ligand by CO, PMe_3, or CH_3CN, all of which are rapid for **1**, is not observed, even at elevated

(19) Kitajima, N.; Tolman, B. W. *Prog. Inorg. Chem.* **1995**, *43*, 419−531.

(20) Trofimenko, S. *Scorpionates: The Coordination Chemistry of Polypyrazolylborate Ligands*; Imperial College: London, 1999.

(21) For a review of C−H activation by neutral TpRh and TpIr complexes, see: Slugovc, C.; Padilla-Martínez, I.; Sirol, S.; Carmona, E. *Coord. Chem. Rev.* **2001**, *213*, 129−157.

(22) Some of these results have been communicated: Tellers, D. M.; Bergman, R. G. *J. Am. Chem. Soc.* **2000**, *122*, 954−955.

(23) Oldham, W. J.; Heinekey, D. M. *Organometallics* **1997**, *16*, 467−474.

Scheme 3

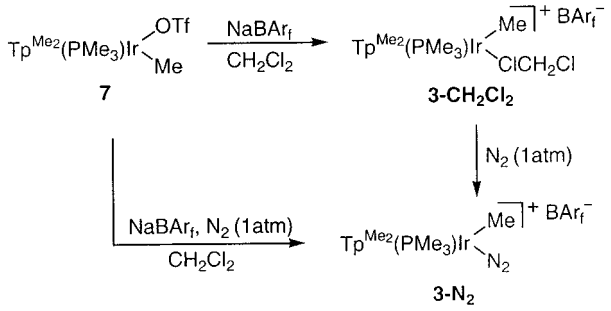

temperatures (>75 °C) and pressures (>5 atm) in dichloromethane solution.

In analogy with the enhanced reactivity of **2-CH_2Cl_2** relative to **1**,[13] we expected that replacing the triflate anion in **7** with the noncoordinating BAr_f anion would produce a more reactive species. Accordingly, treatment of a dichloromethane solution of triflate **7** with $NaBAr_f$ under an *argon* atmosphere resulted in the quantitative formation of $[Tp^{Me_2}(PMe_3)Ir(Me)CH_2Cl_2][BAr_f]$ (**3-CH_2Cl_2**) (Scheme 3). Compound **3-CH_2Cl_2** is thermally sensitive, and as a result, attempts to isolate it have been unsuccessful. Confirmation of this assignment was obtained by low-temperature ^{13}C NMR spectroscopy, where at −80 °C in CH_2Cl_2 a triplet at 62.4 ppm ($^1J_{C-H}$ = 186 Hz) is observed assigned to the carbon atom on the dichloromethane molecule bound to the cationic iridium center.[24−26] Exchange with the bulk solvent becomes fast on the NMR time scale at approximately −20 °C. For $[Cp^*(PMe_3)Ir(CH_2Cl_2)Me][BAr_f]$, attempts to observe the bound dichloromethane were unsuccessful even at −80 °C, presumably because exchange is rapid even at this low temperature.

The thermal sensitivity of **3-CH_2Cl_2** prompted us to explore whether other dative ligands could stabilize the cationic $[Tp^{Me_2}(PMe_3)IrMe]^+$ fragment without drastically attenuating its reactivity. Dinitrogen effectively serves this purpose. When **3-CH_2Cl_2** is placed under N_2 (1 atm), displacement of CH_2Cl_2 occurs in less than 5 min to generate the isolable, thermally stable dinitrogen complex **3-N_2** (Scheme 3). Alternatively, **3-N_2** can be isolated in 74% yield by treating a dichloromethane solution of triflate **7** with $NaBAr_f$ under 1 atm of N_2 (Scheme 3). Compound **3-N_2** exhibits a strong infrared absorption at 2225 cm^{-1} (CH_2Cl_2) assigned to the N≡N stretch. Substitution of $^{14}N_2$ by $^{15}N_2$ produces the expected isotopic shift in the infrared spectrum to 2151 cm^{-1}. This infrared behavior compares well with that of $Tp^{Me_2}Ir(Ph)_2N_2$ (2190 cm^{-1}, Nujol) reported by Carmona and co-workers.[27] Complex **3-N_2** was further characterized by single-crystal X-ray diffraction (Figure 2). Despite the fact that iridium was one of the first metals found to coordinate N_2,[28] to our knowledge **3-N_2** is the first structurally characterized monomeric iridium dinitrogen complex to be reported. Two dimeric iridium dinitrogen complexes have been verified crystallographically.[27,29] Unfortunately, disorder in the Me and N_2 ligand positions in **3-N_2** prevented the determination of exact bond lengths or angles.

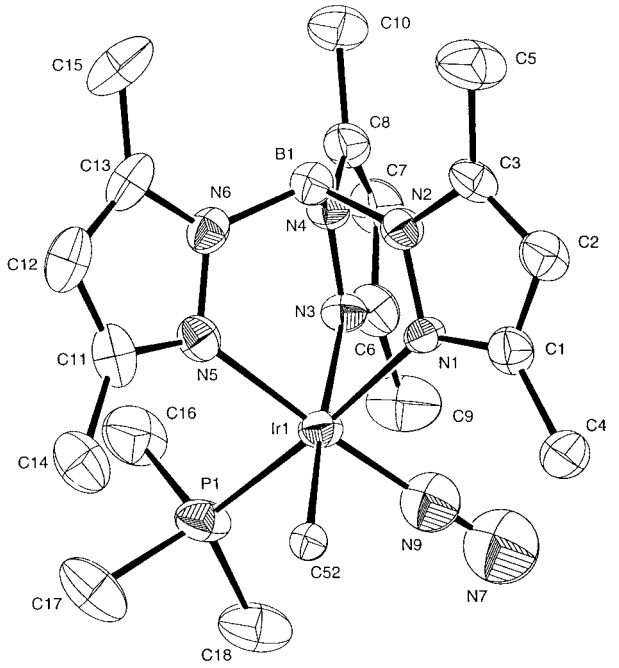

Figure 2. ORTEP diagram of the major component of the cationic portion of $[Tp^{Me_2}(PMe_3)IrMeN_2][BAr_f]$ (**3-N_2**). Thermal ellipsoids are shown at the 50% probability level. Hydrogen atoms have been omitted for clarity.

Spectroscopic Observation of $[Cp^*(PMe_3)IrMe(N_2)][BAr_f]$. The affinity for dinitrogen over dichloromethane exhibited by $[Tp^{Me_2}(PMe_3)IrMe]^+$ was surprising considering the pentamethylcyclopentadienyl analogue, $[Cp^*(PMe_3)IrMe]^+$, preferably binds dichloromethane under identical conditions. This observation provided motivation to explore whether $[Cp^*(PMe_3)IrMe(N_2)][BAr_f]$ (**2-N_2**) could be generated by subjecting **2-CH_2Cl_2** to high dinitrogen pressures. Placing a high-pressure NMR tube containing a CD_2Cl_2 solution of **2-CH_2Cl_2** under 8 atm of dinitrogen results in ^1H and $^{31}P\{^1H\}$ NMR spectroscopic resonances that are slightly shifted with respect to those of the starting dichloromethane complex.[30] We attribute this shift to the establishment of a rapid equilibrium between **2-CH_2Cl_2** and **2-N_2** (eq 2) (vide infra). After venting the NMR tube, the ^1H and $^{31}P\{^1H\}$ NMR spectra indicate complete reversion to **2-CH_2Cl_2**.

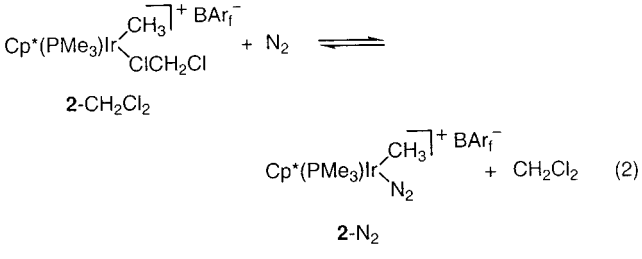

Conclusive spectroscopic evidence for the formation of a dinitrogen complex was obtained by high-pressure infrared spectroscopy. Exposure of **2-CH_2Cl_2** to 10−40 atm of N_2 resulted in observation of an IR absorbance at 2207 cm^{-1}, assigned to the N≡N stretching mode of **2-N_2** (Figure 3).[30] This peak is red-shifted with respect

(24) Free CH_2Cl_2: δ 54 ppm ($^1J_{C-H}$ = 180 Hz).
(25) Vincent-Huhmann, J.; Scott, B. L.; Kubas, G. J. *J. Am. Chem. Soc.* **1998**, *120*, 6808−6809.
(26) Peng, T.; Winter, C. H.; Gladysz, J. A. *Inorg. Chem.* **1994**, *33*, 2534−2542.
(27) Gutiérrez-Puebla, E.; Monge, A.; Nicasio, M. C.; Pérez, P. J.; Poveda, M. L.; Carmona, E. *Chem. Eur. J.* **1998**, *4*, 2225−2236.

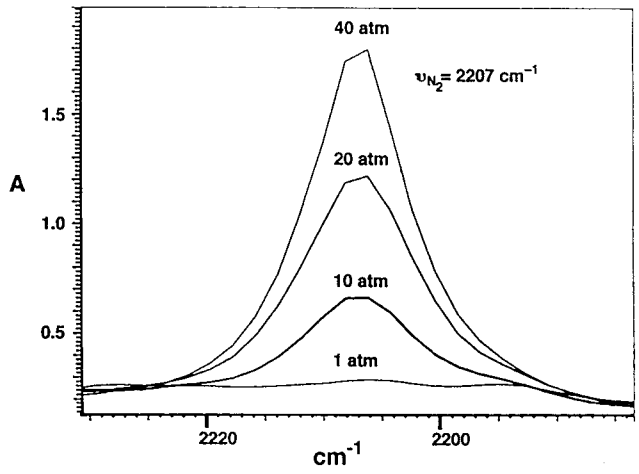

Figure 3. Infrared spectra of [Cp*(PMe$_3$)IrMe][BAr$_f$] in CH_2Cl_2 at various N_2 pressures.

to the dinitrogen absorbance in **3-N$_2$** (2225 cm^{-1}). N_2 coordination to **2** is completely reversible; the absorbance disappeared when N_2 pressure is removed and returns when nitrogen pressure is reintroduced. $^{31}P\{^1H\}$ NMR spectroscopic analysis of an aliquot of this mixture after venting the cell indicated that **2-CH$_2$Cl$_2$** had not decomposed.

Reaction of 3-N$_2$ with Dative Ligands. The dinitrogen ligand in **3** is a better leaving group than the triflate anion and as a result is readily displaced by dative ligands in dichloromethane solution. Treating **3-N$_2$** with CO, CH_3CN, or $AsPh_3$ yields [Tp^{Me_2}(PMe$_3$)IrMe(L)][BAr$_f$] (L = CO (77%), CH_3CN (83%), $AsPh_3$ (99%); $t_{1/2}$ < 5 min) (eq 3).

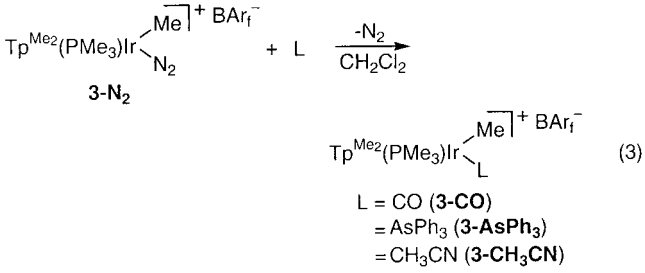

An interesting deviation in the reactivity of **3-N$_2$** is observed with PMe_3. Instead of the expected bisphosphine adduct, [Tp^{Me_2}(PMe$_3$)$_2$IrMe][BAr$_f$], the reaction of **3-N$_2$** with PMe_3 in dichloromethane produces Tp^{Me_2}(PMe$_3$)IrMe(Cl) (**8**) and the phosphonium salt [Me$_3$PCH$_2$Cl][BAr$_f$] ($t_{1/2}$ = 5 min, 25 °C) (eq 4).

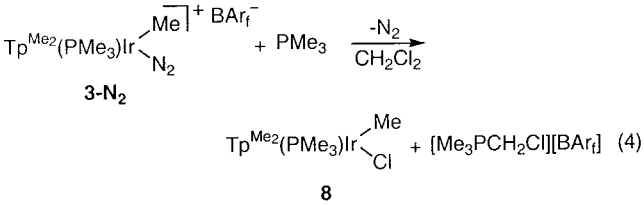

Performing the reaction with PMe$_3$-d_9 and **3-N$_2$** in CH_2Cl_2 yields Tp^{Me_2}(PMe$_3$-d_0)IrMe(Cl)and [Me$_3$PCH$_2$Cl-d_9][BAr$_f$], demonstrating that the phosphonium salt is generated from added phosphine. In CD_2Cl_2 solution, only Tp^{Me_2}(PMe$_3$)IrMe(Cl) and [Me$_3$PCD$_2$Cl][BAr$_f$] are observed. This is consistent with the solvent being the source of "CH_2Cl^+" (i.e., not the iridium-CH_3). In a control experiment, dissolution of PMe_3 in CH_2Cl_2 results in the formation of [Me$_3$PCH$_2$Cl][Cl], but the reaction is very slow (25 °C, $t_{1/2}$ = 10 days).[31] This demonstrates that [Tp^{Me_2}(PMe$_3$)IrMe]$^+$ dramatically accelerates the rate of nucleophilic attack on dichloromethane.

C−H Bond Activation by 3-N$_2$. In contrast to triflate **7**, compound **3-N$_2$** reacts with the C−H bonds of benzene and aldehydes. Reaction of **3-N$_2$** with 1 equiv of benzene in CH_2Cl_2 under a dinitrogen atmosphere produces CH_4 and [Tp^{Me_2}(PMe$_3$)IrPh(N$_2$)][BAr$_f$] (**9**) (76%, $t_{1/2}$ = 3 h) (eq 5).

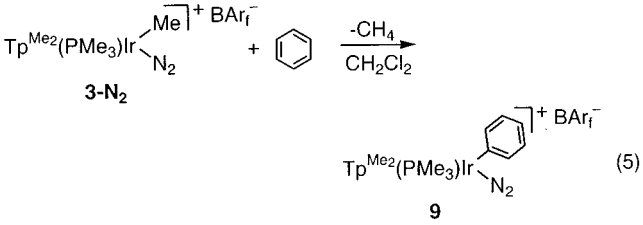

Complex **9** exhibits a strong infrared stretch at 2236 cm^{-1}, which we attribute to iridium-bound N_2. In the ^1H NMR spectrum (CD_2Cl_2) of **9**, five phenyl C−H bond resonances are observed. This is likely the result of hindered rotation about the Ir−Ph bond, as seen in other TpIr systems.[27,32]

A single-crystal X-ray diffraction study of **9** was performed due to the disorder in the structure of **3-N$_2$**. An ORTEP diagram of this molecule is shown in Figure 4. Selected bonding parameters are displayed in Table 2, and the data collection parameters for **9** are presented in Table 5. As would be predicted by the inequivalent aromatic resonances in the ^1H NMR spectrum, the phenyl moiety in **9** lies in the wedge created by the pyrazole groups of the Tp^{Me_2} ligand. This orientation likely minimizes interactions with the pyrazole moieties and prevents Ir−phenyl rotation. The N≡N bond length in the dinitrogen ligand of **9** (1.095(6) Å) is slightly shorter than that observed in the two dimeric iridium dinitrogen complexes (1.13(3) Å[27] and 1.176(13) Å[29]). This bond length is identical to that observed in free N_2 (1.09 Å),[33] demonstrating that the extent of backbonding into the N_2 antibonding orbitals is negligible.

The reaction of **3-N$_2$** with benzene is substantially slower than that observed with the Cp* analogue **2**.[34] A similar difference in reaction rates is observed with aldehydes. Treatment of **3-N$_2$** with acetaldehyde and *p*-tolualdehyde results in formation of the "O-bound" aldehyde complexes [Tp^{Me_2}(PMe$_3$)IrMe(η^1-OC(H)Me)][BAr$_f$] (**10**) and [Tp^{Me_2}(PMe$_3$)IrMe(η^1-OC(H)Tol)][BAr$_f$] (**11**), respectively (Scheme 4). Although the aldehydes

(28) Karsch, H. H. *Phosphorus Sulfur* **1982**, *12*, 217−225.
(29) Collman, J. P.; Kubota, M.; Vastine, F. D.; Sun, J. Y.; Kang, J. W. *J. Am. Chem. Soc.* **1968**, *90*, 5430−5437.
(30) Lee, D. W.; Kaska, W. C.; Jensen, C. M. *Organometallics* **1998**, *17*, 1−3.
(31) See Experimental Section for details.
(32) Ferrari, A.; Polo, E.; Rüegger, H.; Sostero, S.; Venanzi, L. M. *Inorg. Chem.* **1996**, *35*, 1602−1608.
(33) Cohen, J. D.; Mylvaganam, M.; Fryzuk, M. D.; Loehr, T. M. *J. Am. Chem. Soc.* **1994**, *116*, 9529−9534.
(34) The Cp* analogue reacts with benzene at −30 °C ($t_{1/2}$ = 5 min). Complex **3-CH$_2$Cl$_2$** reacts with C_6H_6 at 25 °C to produce [Tp^{Me_2}(PMe$_3$)IrPh(CH$_2$Cl$_2$)][BAr$_f$] ($t_{1/2}$ = 15 min). Like **3-CH$_2$Cl$_2$**, this complex is thermally sensitive, preventing its isolation.

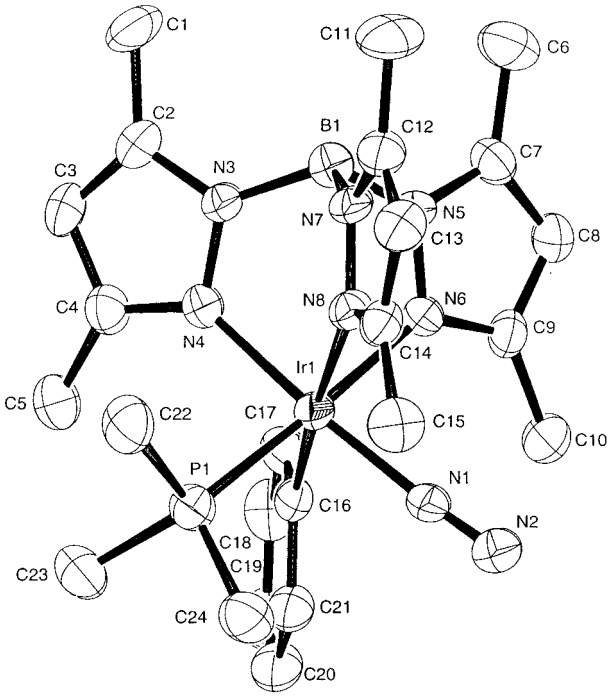

Figure 4. ORTEP diagram of the cationic portion of $[Tp^{Me_2}(PMe_3)IrPhN_2][BAr_f]$. Thermal ellipsoids are shown at the 50% probability level. Hydrogen atoms have been omitted for clarity.

are bound directly to iridium, the aldehyde C−H bonds are completely unreactive at room temperature. The "O-bound" assignment (vs an "η^2 C=O-bound" structure) is based on NMR and IR spectroscopic data.[35−37] As demonstrated by the data in Table 3, the ^1H and $^{13}C\{^1H\}$ NMR chemical shifts of the aldehyde complexes are similar to those of the free aldehyde.[38−42] An η^2-aldehyde complex would exhibit NMR resonances shifted significantly upfield from the corresponding free aldehyde.[41] Furthermore, no phosphorus coupling to the aldehydic protons of **10** and **11** is observed, as would be predicted for an η^2-aldehyde ligand.

While complexes **10** and **11** are stable at room temperature, the aldehydic C−H bond is cleaved at elevated temperatures (Scheme 4). Thermolysis of **10** at 75 °C in dichloromethane results in liberation of methane and formation of the methyl carbonyl species $[Tp^{Me_2}(PMe_3)IrMe(CO)][BAr_f]$ (**3-CO**) (77%, $t_{1/2}$ = 3 h). Similarily, the tolyl carbonyl species $[Tp^{Me_2}(PMe_3)Ir(CO)Tol][BAr_f]$ (**12**) is obtained after heating dichloromethane solutions of **11** at 105 °C (88%, $t_{1/2}$ = 4 h).[43] Four inequivalent tolyl C−H bond resonances are

(35) For examples of TpMo and TpW aldehyde complexes, see refs 36 and 37.

(36) Schuster, D. M.; White, P. S.; Templeton, J. L. *Organometallics* **2000**, *19*, 1540−1548.

(37) Caldarelli, J. L.; Wagner, L. E.; White, P. S.; Templeton, J. L. *J. Am. Chem. Soc.* **1994**, *116*, 2878−2888.

(38) For a discussion of characterization and bonding modes of transition metal-aldehyde complexes, see refs 39−42.

(39) Gladysz, J. A.; Boone, B. J. *Angew. Chem., Int. Ed. Engl.* **1997**, *36*, 550−583.

(40) Lenges, C. P.; Brookhart, M.; White, P. S. *Angew. Chem., Int. Ed.* **1999**, *38*, 552−554.

(41) Faller, J. W.; Ma, Y. *J. Am. Chem. Soc.* **1991**, *113*, 1579−1586.

(42) Cicero, R. L.; Protasiewicz, J. D. *Organometallics* **1995**, *14*, 4792−4798.

(43) For aldehyde activation by a $Tp^{Me_2}Ir$ complex see: Gutierrez-Puebla, E.; Monge, A.; Paneque, M.; Poveda, M. L. Salazar, V.; Carmona, E. *J. Am. Chem. Soc.* **1999**, *121*, 248−249.

Table 2. Selected Intramolecular Distances and Angles for $[Tp^{Me_2}(PMe_3)IrPh(N_2)][BAr_f]$ (9)

	Distance (Å)		
Ir−N(1)	1.950(5)	Ir−N(4)	2.028(6)
Ir−C(16)	2.098(7)	Ir−N(6)	2.115(4)
Ir−P(1)	2.289(2)	Ir −N(8)	2.227(4)
N(1)−N(2)	1.095(6)		
	Angles (deg)		
N(1)−Ir(1)−C(16)	89.7(2)	N(4)−Ir(1)−N(6)	84.0(2)
C(16)−Ir(1)−P(1)	92.8(1)	N(6)−Ir(1)−N(8)	84.9(2)
P(1)−Ir(1)−N(1)	92.4(1)	N(8)−Ir(1)−N(4)	91.1(2)

Table 3. Partial List of NMR Chemical Shifts Used in Assigning the Structures of Aldehyde Complexes 10 and 11

compound	δ O=C(*H*)R[a]	δ O=*C*(H)R[b]
acetaldehyde	9.77	199.7
$[Tp^{Me_2}PMe_3(Me)Ir(O{=}C(H)Me)][BAr_f]$ (**10**)	9.23	223.7
p-tolualdehyde	9.72	192.2
$[Tp^{Me_2}PMe_3(Me)Ir(O{=}C(H)Tol)][BAr_f]$ (**11**)	9.18	207.6

[a] 500 MHz, CD_2Cl_2, 25 °C [b] 125 MHz, CD_2Cl_2, 25 °C

observed in the ^1H NMR spectrum of **12**, due again to hindered rotation of the aryl group. We were unable to observe coalescence of these resonances by ^1H NMR spectroscopy (115 °C, 1,2-dichloroethane-d_4).

In contrast to **1** and **2**, **3-N_2** does not react with the C−H bonds of saturated alkanes such as methane, ethane, pentane, and cyclopropane. For example, when a CD_2Cl_2 solution of **3-N_2** is placed under an atmosphere of $^{13}CH_4$, no incorporation of the isotopic label into the iridium complex is observed after heating at 45 °C for 2 days, at which point **3-N_2** decomposes. Furthermore, addition of an excess of ethane to CD_2Cl_2 solutions of **3-N_2** does not produce $[Tp^{Me_2}(PMe_3)IrH(CH_2CH_2)][BAr_f]$.[44]

Reaction of 3-N_2 with H_2. As described in the Introduction, the design of a system capable of catalytically dehydrogenating alkanes would potentially involve a metal hydride intermediate. We therefore examined the reaction of **3-N_2** with H_2. Exposing a degassed CD_2Cl_2 solution of **3-N_2** to an atmosphere of H_2 for 3 h results in the formation of $[Tp^{Me_2}(PMe_3)IrH(CD_2Cl_2)][BAr_f]$. This compound is characterized by a resonance at −21.60 ppm (d, $^2J_{P-H}$ = 20 Hz). Exposing this solution to N_2 results in growth of a new hydride resonance at −18.80 (d, $^2J_{P-H}$ = 19 Hz, 1H, Ir-*H*) with concomitant loss of the resonance at −21.60 ppm. We attribute this resonance to the hydride ligand of the new complex $[Tp^{Me_2}(PMe_3)IrH(N_2)][BAr_f]$ (**13**). An infrared absorbance at 2231 cm^{-1} assigned to the N_2 stretch and an absorbance at 2205 cm^{-1} assigned to the Ir−H stretch are observed for **13**. Substitution of $^{14}N_2$ for $^{15}N_2$ produces the expected isotopic shift of the former absorption in the infrared spectrum to 2157 cm^{-1} and no change in the stretch at 2205 cm^{-1}.

Preparative amounts of **13** can be obtained by placing degassed CH_2Cl_2 solutions of **3-N_2** under 1 atm of H_2 and stirring for 3 h (Scheme 5). In this case, mixtures of $[Tp^{Me_2}(PMe_3)IrH(CH_2Cl_2)][BAr_f]$ and the known hydrido-dihyrogen complex $[Tp^{Me_2}(PMe_3)IrH(H_2)][BAr_f]$[45]

(44) Alías, F. M.; Poveda, M. L.; Sellin, M.; Carmona, E. *J. Am. Chem. Soc.* **1998**, *120*, 5816−5817.

(45) Oldham, W. J.; Hinkle, A. S.; Heinekey, D. M. *J. Am. Chem. Soc.* **1997**, *119*, 11028−11036.

Scheme 4

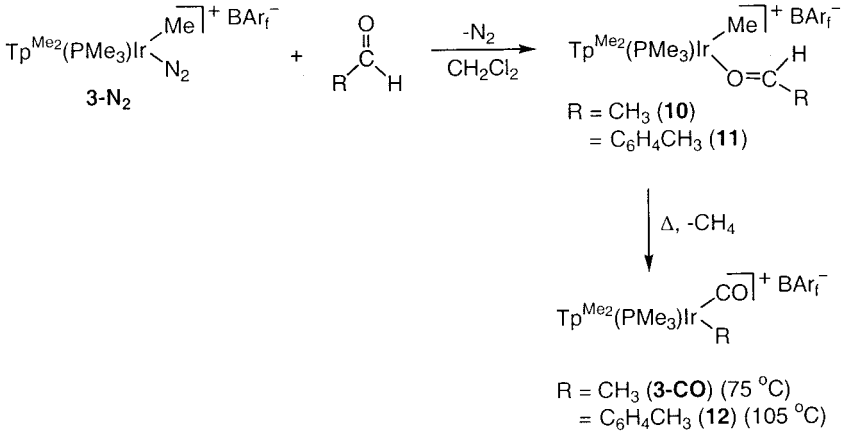

are obtained. Placing this mixture under 40 atm of N_2 results in clean conversion to $[Tp^{Me_2}(PMe_3)IrH(N_2)][BAr_f]$ (**13**) in 64% yield. Analytically pure material was obtained by crystallization from CH_2Cl_2/pentane. Unfortunately, crystals suitable for X-ray analysis could not be grown.

Consistent with the increased steric bulk around the metal, **13** is remarkably stable compared to the Cp* analogue.[18] Decomposition is not observed. This stability is accompanied by reduced reactivity with hydrocarbons. Treating solutions of this compound with hydrocarbons (R−H) does not result in the liberation of hydrogen and formation of $[Tp^{Me_2}(PMe_3)IrR(N_2)][BAr_f]$, nor does the hydrido complex catalyze hydrogen/deuterium exchange, as is observed in the Cp* case.[18,46]

Discussion

Reactivity of $Tp^{Me_2}(PMe_3)IrMeOTf$. Our reactivity studies with the Cp* complexes **1** and **2** demonstrated that the triflate complex **1** and the CD_2Cl_2/borate salt **2** lead to common or similar cationic Ir intermediates via dissociation of triflate or dichloromethane.[17,47−53] We therefore hypothesized that replacing the Cp* ligand with the more sterically encumbering Tp^{Me_2} ligand (cone angle = 276° vs 182° for Cp*)[19] would promote dissociation of the leaving group and facilitate formation of the unsaturated intermediate thought to be responsible for hydrocarbon C−H bond activation.[54]

Triflate **7** was synthesized by a straightforward route from $Tp^{Me_2}(PMe_3)IrH_2$. Surprisingly, **7** did not react with a variety of hydrocarbons and dative ligands. From this lack of reactivity we concluded that triflate dissociation from **7** is substantially slower than it is in the corresponding Cp* complex. We had predicted quite the opposite: the larger coordination sphere occupied by the Tp^{Me_2} ligand should facilitate loss of the triflate leaving group.[55,56] This lack of reactivity must be the result of a difference in the electronic character of the Tp^{Me_2} and Cp* ligands. In a search for precedent, a survey of the Tp and Tp^{Me_2} literature revealed different and sometimes conflicting reports on the relative electron-donating properties of the Cp and Cp* vs Tp and Tp^{Me_2} ligands toward different metals.[57] In several cases, the Tp or Tp^{Me_2} ligand is claimed to be a stronger electron donor than Cp or Cp*. This discrepancy encouraged us to focus more specifically on the electronic differences between Tp^{Me_2} and Cp* bound to iridium.

Infrared spectroscopy often provides a reliable measure of electron density at a metal center, especially for metal carbonyl and N_2 complexes.[58] A table of infrared data for a series of Tp/Tp^{Me_2} and Cp/Cp* iridium complexes is provided in Table 4.[59−66] In all cases, the CO and N_2 stretches of the Cp/Cp* compounds are red-shifted with respect to the Tp/Tp^{Me_2} complexes. These data clearly indicate a *less* electron rich metal center in the Tp^{Me_2} case. Further support for this difference was obtained by examining the proton-transfer equili-

(46) H/D exchange reactions were attempted with c-C_6D_{12}/CH_4 and C_6D_6. Small amounts of CH_3D (<5%) were observed after extended heating (2 days) of **13** and C_6D_{12}/CH_4 at 75 °C along with decomposition.

(47) An extensive amount of work has recently appeared on C−H activation by cationic late transition metals. See refs 48−53.

(48) Stahl, S. S.; Labinger, J. A.; Bercaw, J. E. *J. Am. Chem. Soc.* **1996**, *118*, 5961.

(49) Johansson, L.; Ryan, O. B.; Tilset, M. *J. Am. Chem. Soc.* **1999**, *121*, 1974.

(50) Johansson, L.; Tilset, M.; Labinger, J. A.; Bercaw, J. E. *J. Am. Chem. Soc.* **2000**, *122*, 10846−10855.

(51) Johansson, L.; Tilset, M. *J. Am. Chem. Soc.* **2001**, *123*, 739−740.

(52) Fang, X.; Scott, B. L.; Watkin, J. G.; Kubas, G. *Organometallics* **2000**, *19*, 4193.

(53) Peters, R. G.; White, S.; Roddick, D. M. *Organometallics* **1998**, *17*, 4493−4499.

(54) Krogh-Jespersen, K.; Czerw, M.; Kanzelberger, M.; Goldman, A. S. *J. Chem. Inf. Comput. Sci.* **2001**, *41*, 56−63.

(55) Support for dissociative loss of the triflate ligand can be found in ref 56.

(56) Tellers, D. M.; Bergman, R. G., Tellers, D. M.; Bergman, R. G. *Can. J. Chem.* Accepted for publication.

(57) Tellers, D. M.; Skoog, S. J.; Gunnoe, T. B.; Harman, W. D.; Bergman, R. G. *Organometallics* **2000**, *19*, 2428−2432.

(58) Hunter, A. D.; Mozol, V.; Tsai, S. D. *Organometallics* **1992**, *11*, 2251−2262.

(59) Ball, R. G.; Ghosh, C. K.; Hoyano, J. K.; McMaster, A. D.; Graham, W. G. *J. Chem. Soc., Chem Commun.* **1989**, 341−342.

(60) Hoyano, J. K.; Graham, W. G. *J. Am. Chem. Soc.* **1982**, *104*, 3723−3724.

(61) Fernandez, M. J.; Rodriguez, M. J.; Oro, L. A. *J. Organomet. Chem.* **192**, *438*, 337−342.

(62) Shapley, J. R.; Adair, P.; Lawson, R. J.; Pierpoint, C. G. *Inorg. Chem.* **1982**, *21*, 1701−1709.

(63) Gutiérrez-Puebla, E.; Monge, A.; Nicasio, M. C.; Perez, P. J.; Poveda, M. L.; Rey, L.; Ruiz, C.; Carmona, E. *Inorg. Chem.* **1998**, *37*, 4538−4546.

(64) Bell, T. W.; Haddleton, D. M.; McCamley, A.; Partridge, M. G.; Perutz, R. N.; Willner, H. *J. Am. Chem. Soc.* **1990**, *112*, 9212−9226.

(65) Ciriano, M. A.; Fernández, M. J.; Modrego, J.; Rodríguez, M. J.; Oro, L. A. *J. Organomet. Chem.* **1993**, *438*, 337−342.

(66) Szajek, L. P.; Lawson, R. J.; Shapley, J. R. *Organometallics* **1991**, *10*, 357−361.

Scheme 5

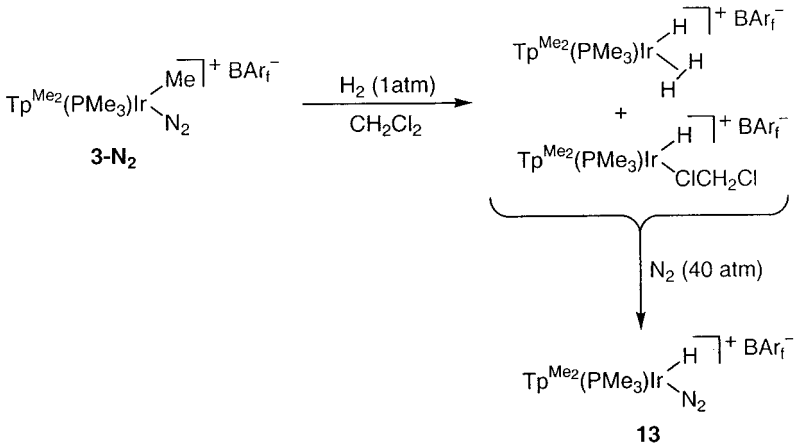

bration of $Tp^{Me_2}(PMe_3)Ir(H)_2H^+OTf^-$ (**14**)[45] and Cp*-$(PMe_3)Ir(H)_2$ (**15**) (eq 6).[67]

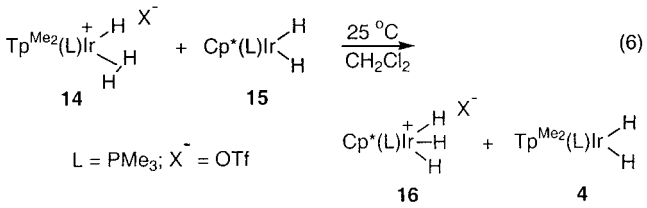

(6)

Treatment of a CD_2Cl_2 solution of **14** with a CD_2Cl_2 solution of **15** results in the quantitative formation of $Cp^*(PMe_3)Ir(H)_3^+OTf^-$ (**16**) and $Tp^{Me_2}(PMe_3)Ir(H)_2$ (**4**), as determined by ^1H and $^{31}P\{^1H\}$ NMR spectroscopy. Thus, the equilibrium lies heavily in favor of the protonated and therefore more strongly basic Cp* complex. Finally, the relative Ir−O bond lengths in triflate **7** and its Cp* analogue **1** are consistent with **7** having the more electrophilic metal center (vide supra). The above results are all consistent with a stronger cation(iridium)/anion(triflate) interaction, which has the effect of slowing the rate of triflate dissociation. The larger barrier to ionization disfavors formation of the key intermediate that reacts with C−H bonds or Lewis bases.

It should be mentioned that the Cp/Cp* and Tp/Tp^{Me_2} ligands interact with the iridium center in fundamentally different ways. The Tp ligand possesses relatively hard nitrogen σ donors, while the Cp ligand possesses relatively soft carbon π donors. Furthermore, the Tp ligand generally enforces an octahedral geometry about the metal center.[68−71] These differences may contribute to the observed differences in reactivity (i.e., the rate of triflate loss) between **1** and **7**. Despite this, we feel that the experimentally confirmed electronic differences between the two ligands described here provide a simple, straightforward explanation for our observations.

Table 4. Summary of the Infrared Absorption Frequencies for Some Iridium Cyclopentadienyl and Hydridotris(pyrazolyl)borate Complexes

compound	data (solvent)	ref
$Tp^{Me_2}Ir(CO)_2$	ν_{CO} = 2039, 1960 cm^{-1} (hexanes)	59
$Cp^*Ir(CO)_2$	ν_{CO} = 2020, 1953 cm^{-1} (hexanes)	60
$Tp(H)_2Ir(CO)$	ν_{CO} = 2020 cm^{-1} (CH_2Cl_2)	61
$Cp(H)_2Ir(CO)$	ν_{CO} = 2002 cm^{-1} (CH_2Cl_2)	62
$Tp^{Me_2}Ir(C_2H_4)CO$	ν_{CO} = 1990 cm^{-1} (Nujol)	63
$TpIr(C_2H_4)CO$	ν_{CO} = 2000 cm^{-1} (cyclohexane)	65
$CpIr(C_2H_4)CO$	ν_{CO} = 1980 cm^{-1} (cyclohexane)	66
$Tp^{Me_2}(C_2H_3)Ir(H)CO$	ν_{CO} = 2020 cm^{-1} (petroleum ether)	63
$Cp(C_2H_3)Ir(H)CO$	ν_{CO} = 2021 cm^{-1} (CO matrix)	64
$[Tp^{Me_2}(PMe_3)IrMe(CO)][BAr_f]$	ν_{CO} = 2060 cm^{-1} (KBr)	a
$[Cp^*(PMe_3)IrMe(CO)][BAr_f]$	ν_{CO} = 2035 cm^{-1} (KBr)	57
$[Tp^{Me_2}(PMe_3)IrMe(N_2)][BAr_f]$	ν_{NN} = 2225 cm^{-1} (CH_2Cl_2)	a
$[Cp^*(PMe_3)IrMe(N_2)][BAr_f]$	ν_{NN} = 2207 cm^{-1} (CH_2Cl_2)	a

[a] This work.

Reactivity of $[Tp^{Me_2}(PMe_3)IrMe(N_2)][BAr_f]$ toward Dative Ligands. In an attempt to generate a more reactive complex, metathesis of the triflate ligand with the BAr_f anion in CH_2Cl_2 under N_2 was performed. Instead of obtaining the expected dichloromethane complex, we isolated the dinitrogen complex, **3-N_2**. Structural characterization of **3-N_2** was also performed since there are surprisingly few iridium dinitrogen complexes.[27−29,72−81]

The affinity for N_2 over CH_2Cl_2 exhibited by the cationic iridium center in **3** is in direct contrast to that of the Cp* analogue **2**, where reversible binding to N_2 is observed only at elevated N_2 pressures (Figure 3). It has recently been noted that CH_2Cl_2 is a better σ donor and a poorer π acceptor than N_2.[82] It is therefore surprising that the more electron rich Cp* compound **2**

(67) Heinekey, D. M.; Hinkle, A. S.; Close, J. D. *J. Am. Chem. Soc.* **1996**, *118*, 5353−5361.
(68) Curtis, M. D.; Shiu, K.-B. *Inorg. Chem.* **1985**, *24*, 1213−1218.
(69) Curtis, M. D.; Shiu, K.; Butler, W. M.; Huffman, J. C. *J. Am. Chem. Soc.* **1986**, *108*, 3335−3343.
(70) Curtis, M. D.; Shiu, K.-B.; Butler, W. M. *J. Am. Chem. Soc.* **1986**, *108*, 1550−1561.
(71) Rüba, E.; Simanko, W.; Mereiter, K.; Schmid, R.; Kirchner, K. *Inorg. Chem.* **2000**, *39*, 382−384.
(72) Please see refs 27−29 and 73−81 for other iridium dinitrogen complexes.
(73) Uguagliati, P.; Deganelo, G.; Busetto, L.; Belluco, U. *Inorg. Chem.* **1969**, *8*, 1625−1630.
(74) Chatt, J.; Melville, D. P.; Richards, R. L. *J. Chem. Soc. A* **1969**, 2841−2844.
(75) Fitzgerald, R. J.; Lin, H.-M. *Inorg. Chem.* **1972**, *11*, 2270−2272.
(76) Blake, D. M. *Chem. Commun.* **1974**, 815−816.
(77) Olgemoeller, B.; Bauer, H.; Beck, W. *J. Organomet. Chem.* **1981**, *213*, C57−C59.
(78) Werner, H.; A., H. *Z. Naturforsch. B: Anorg. Chem.* **1984**, *39b*, 1505−1509.
(79) Bauer, H.; Sheldrick, G. M.; Nagel, U.; Beck, W. *Z. Naturforsch. B: Anorg. Chem.* **1985**, *40b*, 1237−1242.
(80) Bauer, H.; Beck, W. *J. Organomet. Chem.* **1986**, *308*, 73−83.
(81) Goldman, A. S.; Halpern, J. *J. Organomet. Chem.* **1990**, *382*, 237−253.
(82) Toupadakis, A.; Kubas, G. J.; King, W. A.; Scott, B. L.; Huhmann-Vincent, J. *Organometallics* **1998**, *17*, 5315−5323.

Scheme 6

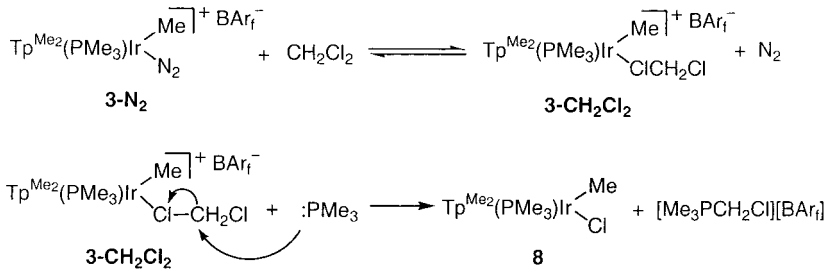

prefers to bind the weaker π acceptor, while the more electron poor compound, **3**, preferentially coordinates the poorer σ donor N_2. We suggest that in this case the steric bulk of the Tp^{Me_2} ligand is important—the larger CH_2Cl_2 molecule has more difficulty fitting into the coordination sphere of the $Tp^{Me_2}Ir$ fragment than the Cp*Ir fragment, an effect that is much reduced with the smaller N_2 molecule.[83] The increased steric demand of the Tp^{Me_2} ligand compared to the Cp* ligand is also demonstrated by the barrier to rotation of an Ir-bound phenyl group: the Tp^{Me_2} systems (**9** and **12**) exhibit hindered rotation, while the analogous Cp* systems exhibit free rotation.[13,16,84]

Replacing the triflate ligand with the noncoordinating BAr_f anion demonstrated that triflate loss from **7** was at least partially responsible for the diminished reactivity in the Tp^{Me_2} system. Dinitrogen, in contrast to triflate, is a good leaving group; Lewis bases readily displace N_2 (eq 3). Further illustration that N_2 readily dissociates is obtained in the reaction of **3-N$_2$** with PMe_3 (eq 4). Instead of the expected phosphine adduct, the phosphonium salt $[Me_3PCH_2Cl][BAr_f]$ and $Tp^{Me_2}(PMe_3)$-IrMe(Cl) are generated. A plausible mechanism to explain formation of these products is illustrated in Scheme 6. Complex **3-N$_2$** is in rapid equilibrium with **3-CH$_2$Cl$_2$**. Subsequent PMe_3 attack on bound CH_2Cl_2 yields the observed products.[85] In this case, the cationic $[Tp^{Me_2}(PMe_3)IrMe]^+$ fragment serves as a Lewis acid, activating the dichloromethane toward nucleophilic attack. Similar Lewis acid-assisted reactions have been observed with rhenium[26,86] and ruthenium.[87] While the preference for PMe_3 attack at the Ir-bound dichloromethane carbon over attack at the iridium center is not completely understood, this reaction provides evidence for the dynamic preequilibrium illustrated in Scheme 6.

Why is the Tp^{Me_2} System Less Reactive Than the Cp* System? Complex **3-N$_2$** is capable of activating the C−H bonds of arenes and aldehydes under moderate conditions, albeit at a slower rate than the corresponding Cp* systems. As we have stated in two previous papers, we are convinced that Tp ligands are poorer electron donors than Cp* toward Ir.[22,57] However, this can lower the relative C−H activation reactivity of the Tp-type systems in two ways: it can increase the energy required for dissociation of the weakly bound dative ligand (OTf^-, CH_2Cl_2, N_2) from the 18-electron Ir center, and/or it can raise the energy of the C−H activation transition state itself. Our most recent low-temperature NMR investigations of the two systems demonstrate that they show a strong difference in dative ligand dissociation rate. As noted in the Results section, we are unable to freeze out separate resonances for bound and free dichloromethane in $[Cp^*(PMe_3)Ir(CH_2Cl_2)]^+$ at −80 °C (indicating that dissociation is relatively rapid even at this temperature), whereas this can be done with the analogous Tp^{Me_2} complex. In $[Tp(PMe_3)Ir(CH_2Cl_2)]^+$, dissociation of CH_2Cl_2 is slow even at mildly elevated temperatures. Since this preequilibrium directly affects the overall rate of the C−H activation reaction, we conclude that it must be an important factor in slowing the process.

Given the fact that compounds such as aldehydes and arenes do ultimately react in the Tp^{Me_2} system, it is perplexing that we see no reaction at all with alkanes even under the most stringent conditions we can reach, short of irreversible decomposition of the complexes. Although this observation is purely qualitative, on the basis of it we continue to believe that there must also be a contribution of electron donor stabilization to the C−H oxidative addition transition state. When the amount of donation is insufficient, as it must be in the Tp^{Me_2} and Tp systems, C−H activation shuts down completely. One other factor to consider is the ease or difficulty of expanding the Ir coordination sphere. Mechanistic and theoretical work provide strong evidence that C−H activation by cationic iridium(III) complexes proceeds through 18 e^-, iridium(V) intermediates.[11,16,88,89] Accordingly, it is likely that the intermediate in the Tp^{Me_2} system is an 18 e^-, seven-coordinate, Ir(V) species of the type shown in Figure 5A. There are few seven-coordinate Tp complexes known, compared to (formally) seven-coordinate Cp complexes.[69,71,90,91] If this reflects the difficulty of expanding the coordination sphere in Tp and Tp^{Me_2} complexes,[92−94]

(83) Support for this hypothesis obtained by utilizing the Tp ligand will be published separately.

(84) Woerpel, K. A.; Bergman, R. G. *J. Am. Chem. Soc.* **1993**, *115*, 7888−7889.

(85) See ref 27 for a description of the reaction of PMe_3 with ethylene in $Tp^{Me_2}(CH_2CH_2)Ir(CHCH_2)H$.

(86) Igau, A.; Gladysz, J. A. *Polyhedron* **1991**, *10*, 1903−1909.

(87) Kulawiec, R. J.; Crabtree, R. H. *Organometallics* **1988**, *7*, 1891−1893.

(88) Klei, S. R.; Bergman, R. G. *J. Am. Chem. Soc.* **2000**, *122*, 1816−1817.

(89) Strout, D. L.; Zaric, S.; Niu, S.; Hall, M. B. *J. Am. Chem. Soc.* **1996**, *118*, 6068−6069.

(90) Skagestad, V.; Tilset, M. *J. Am. Chem. Soc.* **1993**, *115*, 5077−5083.

(91) Tenorio, M. J.; Tenorio, M. A. J.; Puerta, M. C.; Valerga, P. *Inorg. Chim. Acta* **1997**, *259*, 77−84.

(92) The desire to maintain an octahedral geometry has been used to explain why TpM complexes form nonclassical dihydrogen structures whereas the corresponding Cp* complexes will go seven-coordinate and form classical dihydride structures. See the two references immediately following this one.

(93) Gutiérrez-Puebla, E.; Monge, A.; Paneque, M.; Poveda, M. L.; Taboada, S.; Trujillo, M.; Carmona, E. *J. Am. Chem. Soc.* **1999**, *121*, 346−354.

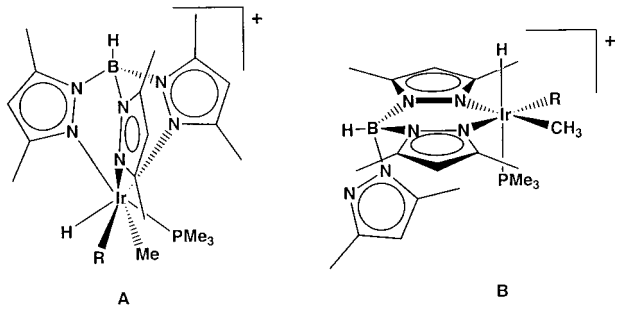

Figure 5. Proposed Ir(V) intermediates in C−H activation by $\mathbf{3}^+$.

this effect may also be important in raising the energy of the C−H oxidative addition transition state. Dechelation of one of the pyrazole arms would provide a means of preventing the necessity of forming a seven-coordinate intermediate (Figure 5B). Such a complex would be analogous to those proposed in neutral Rh(I) C−H activation reactions.[95,96] However, if it were to occur, dechelation would require additional energy input and would also diminish the already relatively poor electron-donating ability of the Tp^{Me_2} ligand.

Conclusion

This work has provided an account of the chemistry of a series of $Tp^{Me_2}Ir(III)$ complexes. A comparison of the relative electron-donating abilities of the Tp and Cp ligand toward iridium has been made, and it was shown that electronic effects play an important role in defining the reactivity of these complexes. In particular, triflate dissociation from $Tp^{Me_2}PMe_3Ir(Me)OTf$ occurs very slowly because the iridium center is more electrophilic than it is in the Cp* complex. Replacement of triflate with BAr_f provides access to a variety of new cationic iridium dinitrogen complexes, $[Tp^{Me_2}PMe_3Ir(R)N_2][BAr_f]$ (R = Me, Ph, H). In the case of R = Me (**3-N$_2$**), C−H activation of benzene and aldehydes occurs, but saturated hydrocarbons fail to react. It is postulated that the inability of the Tp^{Me_2} framework to support a seven-coordinate intermediate, coupled with its poor electron-donating ability, prevents activation of the saturated hydrocarbons. In predicting and interpreting chemistry with the Tp ligand, consideration should be given to the electron-donating abilities of the ligand, not just to its steric properties. A catalytically active dehydrogenation system will require a large, electron-rich, ancillary ligand set.

Experimental Section

General Procedures. General experimental information has been reported elsewhere.[16] All NMR spectra were obtained at room temperature (except where noted) using Bruker AM-400 or DRX-500 MHz spectrometers. ^{11}B NMR spectra were recorded at 160 MHz, and chemical shifts (δ) are reported relative to external $BF_3{\cdot}Et_2O$. ^{15}N NMR spectra were recorded at 50.7 MHz, and chemical shifts (δ) are reported relative to external CH_3NO_2. ^{19}F NMR spectra were recorded at 377 MHz, and chemical shifts (δ) are reported relative to external $CFCl_3$. $^{31}P\{^1H\}$ NMR spectra were recorded at 162 MHz, and chemical shifts (δ) are reported relative to external 85% H_3PO_4. X-ray structural analyses were performed at the UC Berkeley CHEXRAY facility by Dr. Fred Hollander and Dr. Dana Caulder.

Sealed NMR tubes were prepared by attaching the NMR tube directly to a Kontes high-vacuum stopcock via a Cajon Ultra-Torr reducing union and then flame-sealing on a vacuum line. Reactions with gases and low-boiling liquids involved condensation of a calculated pressure of gas from a bulb of known volume into the reaction vessel at −196 °C. Known-volume bulb vacuum-transfers were accomplished with a digital MKS Baratron gauge attached to a vacuum line.

Materials. Unless otherwise noted, reagents were purchased from commercial suppliers and used without further purification. Potassium bromide (Aldrich), Celite (Aldrich), silica gel (Merck 60, 230−400), and silylated silica gel (EM Science, silica gel 60, 63−200 μm) were dried in vacuo at 250 °C for 48 h. Toluene (Fisher) was either distilled from sodium metal under N_2 or passed through a column of activated alumina (type A2, size 12 × 32, Purifry Co.) under nitrogen pressure and sparged with N_2 prior to use.[97] Pentane, hexanes, and benzene (Fisher) were either distilled from purple sodium/benzophenone ketyl under N_2 or passed through a column of activated alumina (type A2, size 12 × 32, Purifry Co.) under nitrogen pressure and sparged with N_2 before use.[97] Diethyl ether and tetrahydrofuran (Fisher) were distilled from purple sodium/benzophenone ketyl under N_2 prior to use. Dichloromethane (Fisher) was either distilled from CaH_2 (Aldrich) under N_2 or passed through a column of activated alumina (type A2, size 12 × 32, Purifry Co.) under nitrogen pressure and sparged with N_2 prior to use.[97] Deuterated solvents (Cambridge Isotope Laboratories) were purified by vacuum-transfer from the appropriate drying agent (Na/Ph_2CO or CaH_2) prior to use.

Trimethylphosphine (Aldrich) was vacuum-transferred from sodium metal prior to use. *N*-Bromosuccinimide was crystallized from water and dried in vacuo for 2 days before use.[98] Tolualdehyde and CCl_4 were dried over 4 Å molecular sieves prior to use. Acetaldehyde was stored over 3 Å sieves at 0 °C. $Tp^{Me_2}(PMe_3)IrH_2$,[23] $[Cp^*(PMe_3)IrMe(CH_2Cl_2)][BAr_f]$,[13] and $NaBAr_f$[99] were prepared according to literature procedures.

$Tp^{Me_2}(PMe_3)IrBr_2$ (5). In a drybox, precooled CCl_4 (20 mL, −20 °C) was added to a vial containing $Tp^{Me_2}(PMe_3)IrH_2$ (1.40 g, 0.0024 mol) and *N*-bromosuccinimide (0.87 g, 0.0048 mol). The resulting green solution was stirred vigorously at 22 °C for 3 h, over which time a light green solid precipitated. The vial was removed from the drybox, and the precipitate was collected on a Buchner funnel, rinsed with ether (5 × 10 mL), and dissolved in a minimum of CH_2Cl_2 (3 mL). The solution was run through a column of silica gel (10 cm × 3 cm) in order to remove the residual succinimide. The light yellow eluent was collected, and the solvent was removed under reduced pressure to yield a yellow solid. Yield: 930 mg, 53%. This material was judged sufficiently pure (>95%) by ^1H NMR spectroscopy for subsequent transformations. Analytically pure material can be obtained by crystallization from CH_2Cl_2/Et_2O. ^1H NMR (400 MHz, $CDCl_3$, 25 °C): δ 5.79 (s, 1H, pyrC*H*), 5.78 (s, 2H, pyrC*H*), 2.85 (s, 3H, pyrCH_3), 2.70 (s, 6H, pyrCH_3), 2.42 (s, 6H, pyrCH_3), 2.33 (s, 3H, pyrCH_3), 1.74 (d, $^2J_{P-H}$ = 10 Hz, 9H, P*Me*$_3$). $^{13}C\{^1H\}$ NMR (125 MHz, CD_2Cl_2, 25 °C): δ 12.8 (s, pyr*C*H$_3$), 13.5 (s, pyr*C*H$_3$), 16.7 (s, pyr*C*H$_3$), 17.3 (d, $^1J_{P-C}$ = 41 Hz, P*Me*$_3$), 18.3 (s, pyr*C*H$_3$), 109.2 (d, $^4J_{P-C}$ = 5 Hz, pyr*C*H), 110.5 (s, pyr*C*H), 144.2 (s, pyrC_q), 145.6 (s, pyrC_q),

(94) Oldham, W. J.; Hinkle, A. S.; Heinekey, D. M. *J. Am. Chem. Soc.* **1997**, *119*, 11028−11036.
(95) Bromberg, S. E.; Yang, H.; Asplund, M. C.; Lian, T.; McNamara, B. K.; Kotz, K. T.; Yeston, J. S.; Wilkens, M.; Frei, H.; Bergman, R. G.; Harris, C. B. *Science* **1997**, *278*, 260−263.
(96) Wick, D. D.; Reynolds, K. A.; Jones, W. D. *J. Am. Chem. Soc.* **1999**, *121*, 3974−3983.
(97) Alaimo, P. J.; Peters, D. W.; Arnold, J.; Bergman, R. G. *J. Chem. Educ.* **2001**, *78*, 64.
(98) Perrin, D. D.; Armarego, W. L. F. *Purification of Laboratory Chemicals*, 3rd ed.; Pergamon Press: Oxford, 1988.

Table 5. Crystal Data Collection and Refinement Parameters for Complexes 3-N_2, 7, and 9

	3-N_2	7	9
empirical formula	$IrCl_3PF_{24}C_{52.5}N_8B_2H_{55}$	$IrSPF_3O_3N_6C_{21}BH_{36}Cl_2$	$IrPF_{24}N_8C_{56}H_{48}B_2$
fw	1605.20	814.52	1533.82
cryst habit	pale yellow plates	yellow blades	yellow prisms
cryst size, mm	0.40 × 0.22 × 0.10	0.16 × 0.12 × 0.06	0.23 × 0.21 × 0.14
cryst syst	monoclinic	monoclinic	monoclinic
lattice type	C-centered	primitive	primitive
a, Å	39.1718(7)	8.8148(1)	12.2962(2)
b, Å	12.9265(2)	15.8021(1)	20.4899(1)
c, Å	26.0390(4)	20.0649(3)	27.0853(3)
β, deg	107.452(1)	92.853(1)	100.130(1)
V, Å^3	12578.0(3)	2791.42(5)	6717.7(1)
space group	*C*2/*c* (#15)	$P2_1/c$ (#14)	$P2_1/c$ (#14)
Z value	8	4	4
D_{calc}, g/cm^3	1.695	1.938	1.516
F_{000}	6056.00	1608.00	3032.00
temp, °C	−128	−120	−108
μ(Mo Kα), cm^{-1}	23.52	51.77	55.86
exposure time, s/frame	10.0	15.0	10.0
$2\theta_{max}$, deg	49.4	49.4	49.4
no. of reflns measd			
total	27 863	13 173	29 792
unique	11 118	4919	11 412
no. observations	7014	3087	7156
no. variables	785	342	880
reflns/param ratio	8.94	9.03	8.13
R^a; R_w^b; R_{all}	0.045; 0.052; 0.077	0.030; 0.032; 0.067	0.030; 0.034; 0.054
GOF indicator	1.52	0.95	1.20
max. resid density, e/Å^3	1.22	0.93	0.72
min. resid density, e/Å^3	−0.93	−1.11	−0.40

^{a} $R = \sum||F_o| - |F_c||/\sum|F_o|$. ^{b} $R_w = [\sum w(|F_o| - |F_o|)^2/\sum w|F_o|^2]^{1/2}$, $w = 1/\sigma^2(F_o)$

155.2 (d, $^3J_{P-C}$ = 4 Hz, pyr*C*$_q$), 154.8 (s, pyr*C*$_q$). $^{31}P\{^1H\}$ NMR (161.9 MHz, CD_2Cl_2, 25 °C): δ −65.7. ^{11}B NMR (160 MHz, CD_2Cl_2, 25 °C): δ −9.86 (d, $^1J_{B-H}$ = 104 Hz). IR (KBr): 3129 (w), 2960 (m), 2922 (m), 2551 (m), 1551 (s), 1449 (s), 1420 (s), 1380 (s), 1309 (m), 1288 (m), 1217 (s), 1065 (s), 1045 (m), 961 (s), 864 (m), 821 (s), 789 (s), 742 (m), 690 (m), 645 (m), 484 (w). MS (EI): *m*/*z* 726 (M^+). Anal. Calcd for $C_{18}H_{31}BBr_2IrN_6$: C, 29.81; H, 4.31; N, 11.59. Found: C, 29.99; H, 4.46; N, 11.42.

Tp^{Me_2}(PMe$_3$)IrMe(Br) (6). To a stirred slurry of **5** (1.40 g, 0.0019 mol) in THF (20 mL) at −40 °C was added MeLi (0.0032 mol, 1.7 equiv, 1.4 M in Et_2O) by syringe. After 2 h at 22 °C, the homogeneous solution was run through a plug of alumina (2 cm × 3 cm) and the solvent was removed under reduced pressure to yield a yellow-orange solid. The solid was dissolved in a minimum of CH_2Cl_2, and the resulting solution was layered with pentane and cooled to −40 °C to afford yellow crystals of Tp^{Me_2}(PMe$_3$)IrMe(Br). Yield: 740 mg, 60%. ^1H NMR (500 MHz, CD_2Cl_2, 25 °C): δ 5.84 (s, 1H, pyrC*H*), 5.80 (s, 1H, pyrC*H*), 5.77 (s, 1H, pyrC*H*), 2.63 (s, 3H, pyrC*H*$_3$), 2.57 (s, 3H, pyrC*H*$_3$), 2.43 (s, 3H, pyrC*H*$_3$), 2.42 (s, 3H, pyrC*H*$_3$), 2.33 (s, 3H, pyrC*H*$_3$), 2.33 (s, 3H, pyrC*H*$_3$), 1.83 (d, $^2J_{P-H}$ = 4 Hz, Ir-*Me*), 1.53 (d, $^2J_{P-H}$ = 10 Hz, P*Me*$_3$). $^{13}C\{^1H\}$ (125 MHz, CD_2Cl_2, 25 °C): δ −27.5 (Ir-*C*H$_3$, $^2J_{P-C}$ = 6 Hz), 13.08 (s, pyr*C*H$_3$), 13.2 (s, pyr*C*H$_3$), 13.7 (s, pyr*C*H$_3$), 15.0 (s, pyr*C*H$_3$), 16.1 (d, $^1J_{P-C}$ = 40 Hz, P*Me*$_3$), 16.6 (s, pyr*C*H$_3$), 17.2 (s, pyr*C*H$_3$), 108.7 (d, $^4J_{P-C}$ = 5 Hz, pyr*C*H), 109.0 (s, pyr*C*H), 109.5 (s, pyr*C*H), 143.8 (s, pyr*C*$_q$), 144.7 (s, pyr*C*$_q$), 145.2 (s, pyr*C*$_q$), 152.3 (s, pyr*C*$_q$), 152.7 (s, pyr*C*$_q$), 153.5 (s, pyr*C*$_q$). $^{31}P\{^1H\}$ NMR (161.9 MHz, CD_2Cl_2, 25 °C): δ −56.9. ^{11}B NMR (160 MHz, CD_2Cl_2, 25 °C): δ −9.72 (d, $^1J_{B-H}$ = 102 Hz). IR (KBr): 2954 (s), 2919 (s), 2527 (m), 1550 (s), 1444 (s), 1416 (s), 1380 (s), 1305 (w), 1285 (w), 1216 (s), 1134 (w), 1063 (s), 1037 (m), 958 (s), 858 (m), 815 (m), 786 (s), 734 (m), 693 (m). MS (EI): *m*/*z* 660 (M^+), 645 ($M^+ - CH_3$). Anal. Calcd for $C_{19}H_{34}BBrIrN_6$: C, 34.55; H, 5.19; N, 12.72. Found: C, 34.81; H, 5.36; N, 12.81.

Tp^{Me_2}(PMe$_3$)IrMe(OTf) (7). CH_2Cl_2 (20 mL) was added to a vial containing **6** (1.30 g, 0.002 mol) and AgOTf (510 mg, 0.002 mol). The brown slurry was shielded from light and stirred for 12 h. The solution was filtered through silanized silica gel, concentrated to ∼1 mL, layered with pentane, and cooled to −40 °C. Light yellow crystals of Tp^{Me_2}(PMe$_3$)IrMe(OTf) were isolated after 24 h. Yield: 630 mg, 42%. ^1H NMR (400 MHz, CD_2Cl_2, 25 °C): δ 5.92(s, 1H, pyrC*H*), 5.78 (s, 2H, pyrC*H*), 2.44 (s, 3H, pyrC*H*$_3$), 2.44 (s, 3H, pyrC*H*$_3$), 2.42 (s, 3H, pyrC*H*$_3$), 2.29 (s, 9H, pyrC*H*$_3$), 2.17 (d, $^3J_{P-C}$ = 3 Hz, Ir-*Me*), 1.49 (d, $^2J_{P-C}$ = 10 Hz, P*Me*$_3$). $^{13}C\{^1H\}$ NMR (125 MHz, CD_2Cl_2, 25 °C): δ −27.9 (d, 3H, $^3J_{P-C}$ = 5 Hz, Ir-*Me*), 13.0 (s, pyr*C*H$_3$), 13.1 (s, pyr*C*H$_3$), 13.6 (s, pyr*C*H$_3$), 13.7 (s, pyrCH$_3$), 15.6 (s, $^4J_{P-C}$ = 2 Hz, pyr*C*H$_3$), 16.3 (d, $^1J_{P-C}$ = 39 Hz, P*Me*$_3$), 16.6 (s, pyr*C*H$_3$), 108.2 (d, $^4J_{P-C}$ = 4 Hz, pyr*C*H), 108.8 (s, pyrCH), 109.9 (s, pyr*C*H), 144.4 (d, $^3J_{P-C}$ = 3 Hz, pyr*C*$_q$), 146.1 (s, pyr*C*$_q$), 146.3 (s, pyr*C*$_q$), 151.7 (d, $^5J_{P-C}$ = 4 Hz, pyr*C*$_q$), 152.9 (s, pyr*C*$_q$), 154.1 (s, pyr*C*$_q$), *C*F$_3$ not observed. $^{31}P\{^1H\}$ NMR (161.9 MHz, CD_2Cl_2, 25 °C): δ −54.0. ^{19}F NMR (376.5 MHz, CD_2Cl_2, 25 °C): δ −75.5. ^{11}B NMR (160 MHz, CD_2Cl_2, 25 °C): δ −9.71 (d, $^1J_{B-H}$ = 100 Hz). IR (KBr): 2979 (m), 2926 (m), 2556 (m), 1551 (s), 1448 (s), 1417 (s), 1384 (m), 1324 (s), 1229 (s), 1203 (s), 1179 (s), 1065 (m), 1008 (s), 960 (m), 863 (w), 826 (w), 782 (m), 691 (w), 637 (s), 518 (w). MS (EI): *m*/*z* 730 (M^+), 715 ($M^+ - CH_3$). Anal. Calcd for $C_{20}H_{34}N_6BIrPO_3SF_3 \cdot 1/4CH_2Cl_2$ (confirmed by ^1H NMR spectroscopy): C, 32.40; H, 4.60; N, 11.20. Found: C, 32.54; H, 4.71; N, 11.11.

Generation of $[Tp^{Me_2}$(PMe$_3$)IrMe(CD_2Cl_2)][BAr_f] (3-CD_2Cl_2) in CD_2Cl_2 Solution. Compound **3-CD_2Cl_2** was always generated immediately prior to use. Typical procedure: in a drybox, an NMR tube was charged with **7** (30.0 mg, 0.041 mmol) and $NaBAr_f$ (36.0 mg, 0.041 mmol). The tube was removed from the drybox and attached to a vacuum line, and CD_2Cl_2 (∼0.6 mL) was added via vacuum-transfer techniques. After thawing, the slurry was shaken for 10 min and then the NaOTf was allowed to settle. The light yellow solution containing $[Tp^{Me_2}$(PMe$_3$)IrMe(CD_2Cl_2)][BAr_f] is stable for approximately 6 h at 298 K. Attempts to isolate this compound were unsuccessful. ^1H NMR (400 MHz, CD_2Cl_2, 25 °C): δ 7.72 (bs, 8H, *o*-BAr_f), 7.56 (bs, 4H, *p*-BAr_f), 6.05 (s, pyrC*H*), 5.92 (s, pyrC*H*), 5.81 (s, pyrC*H*), 2.46 (s, 3H, pyr*Me*), 2.42 (s, 9H, pyr*Me*), 2.35 (s, 3H, pyr*Me*), 2.30 (s, 3H, pyr*Me*), 2.00 (d, $^3J_{P-H}$ = 5 Hz, 3H, Ir-*Me*), 1.53 (d, $^2J_{P-H}$ = 14 Hz, 9H, P*Me*$_3$). $^{13}C\{^1H\}$ NMR (125 MHz, CH_2Cl_2, 25 °C): δ 161.9 (d, $^1J_{B-C}$ = 50 Hz, *i*-BAr_f), 154.1 (s, pyr*C*$_q$), 151.4 (d, $^3J_{P-C}$ = 4 Hz, pyr*C*$_q$), 150.7 (s, pyr*C*$_q$), 148.2 (s, pyr*C*$_q$), 146.4 (s, pyr*C*$_q$), 146.1 (d, $^3J_{P-C}$ = 3 Hz, pyr*C*$_q$), 135.0 (s, *o*-BAr_f), 129.1 (qq, $^2J_{F-C}$ = 31 Hz, $^4J_{F-C}$ = 3 Hz, *m*-BAr_f), 124.8 (q, $^1J_{F-C}$ = 270 Hz, BAr_fCF_3), 117.7 (septet, $^3J_{F-C}$ = 4 Hz, *p*-BAr_f), 110.9 (s, pyr*C*H), 109.5 (s, pyr*C*H), 109.3 (d, $^4J_{F-C}$ = 4 Hz, pyr*C*H), 16.1 (s, pyr*C*H$_3$), 16.0 (s, pyr*C*H$_3$), 15.4 (d, $^1J_{P-C}$ = 40 Hz, P*Me*$_3$), 14.0 (s, pyr*C*H$_3$), 13.5 (s, pyr*C*H$_3$), 12.6 (s, pyr*C*H$_3$), 12.5 (s, pyr*C*H$_3$), −27.1 (d, $^2J_{P-C}$ = 6 Hz, Ir-*Me*). ^{13}C (125 MHz, CH_2Cl_2, −80 °C): δ 62.4 (t, $^1J_{C-H}$ = 186 Hz, *C*H$_2$Cl$_2$). $^{31}P\{^1H\}$ NMR (161.9 MHz, CD_2Cl_2, 25 °C): δ −52.3. ^{19}F NMR (376.5 MHz, CD_2Cl_2, 25 °C): δ −61.0. ^{11}B NMR (160 MHz, CD_2Cl_2, 25 °C): δ −8.7 (s, BAr_f), −11.0 (d, $^1J_{B-H}$ = 97 Hz, Tp^{Me_2}).

[Tp^{Me_2}(PMe$_3$)IrMe(N_2)][BAr_f] (3-N_2). CH_2Cl_2 (10 mL) was added to a vial containing **7** (90.3 mg, 0.12 mmol) and $NaBAr_f$ (110 mg, 0.12 mmol). The solution was stirred for 30 min and filtered through glass fiber filter paper. The solvent was removed under reduced pressure to afford **3-N_2** as an off-white solid. Crystallization from a concentrated CH_2Cl_2 solution layered with pentane at −40 °C produced clear, blocklike crystals of **3-N_2**. Yield: 126 mg, 67%. ^1H NMR (500 MHz, CD_2Cl_2, 25 °C): δ 7.72 (bs, 8H, *o*-BAr_f), 7.56 (bs, 4H, *p*-BAr_f), 6.02 (s, 1H, pyrC*H*), 5.93 (s, 1H, pyrC*H*), 5.88 (s, 1H, pyrC*H*), 2.43 (s, 3H, pyrC*H*$_3$), 2.36 (s, 6H, pyrC*H*$_3$), 2.33 (s, 3H, pyrC*H*$_3$), 2.31 (s, 3H, pyrC*H*$_3$), 1.63 (d, 3H, $^3J_{P-H}$ = 3 Hz, Ir-*Me*), 1.61 (d, 9H, $^2J_{P-H}$ = 11 Hz, Ir-P*Me*$_3$). $^{13}C\{^1H\}$ NMR (CD_2Cl_2, 125 MHz, 25 °C): δ −23.6 (d, $^2J_{P-C}$ = 6 Hz, Ir-*Me*), 12.8 (s, pyr*C*H$_3$), 12.9 (s, pyr*C*H$_3$), 13.7 (s, pyr*C*H$_3$), 14.0 (s, pyr*C*H$_3$), 23.3 (d, $^1J_{P-C}$ = 41 Hz, PMe$_3$), 16.4 (s, pyr*C*H$_3$), 16.8 (s, pyr*C*H$_3$), 109.1

(d, $^4J_{P-C}$ = 4 Hz, pyr*C*H), 109.7 (s, pyr*C*H), 111.6 (s, pyr*C*H), 118.1 (septet, $^3J_{F-C}$ = 4 Hz, *p*-BAr_f), 125.2 (q, $^1J_{F-C}$ = 270 Hz, BAr_fCF_3), 129.48 (qq, $^2J_{F-C}$ = 32 Hz, $^4J_{F-C}$ = 3 Hz, *m*-BAr_f), 135.4 (s, *o*-BAr_f), 146.1 (d, $^3J_{P-C}$ = 3 Hz, pyrC_q), 147.0 (s, pyrC_q), 148.2 (s, pyrC_q), 151.2 (d, $^3J_{P-C}$ = 4 Hz, pyrC_q), 151.6 (s, pyrC_q), 154.0 (s, pyrC_q), 162.4 (q, $^1J_{B-C}$ = 50 Hz, *i*-BAr_f). $^{31}P\{^1H\}$ NMR (161.9 MHz, CD_2Cl_2, 25 °C): δ −47.3. ^{19}F NMR (376.5 MHz, CD_2Cl_2, 25 °C): δ −61.0. ^{11}B NMR (160 MHz, CD_2Cl_2, 25 °C): δ −9.54 (d, $^1J_{B-H}$ = 106 Hz). ^{15}N NMR (50.7 MHz, CD_2Cl_2, 25 °C): δ −49.2 (N_α), −144.4 (N_β). IR (CH_2Cl_2): 2566 (m, B-H), 2225 (s, N_2) cm^{-1}. IR (KBr): 2975 (m), 2929 (m), 2565 (m, B-H), 2227 (s, N_2), 1785 (w), 1611 (s), 1551 (s), 1450 (s), 1422 (s), 1357 (s), 1272 (vs), 1169 (vs), 959 (s), 888 (s), 839 (s), 793 (w), 714 (s), 671 (s). Anal. Calcd for $C_{51}H_{46}B_2PIrN_8F_{24}\cdot CH_2Cl_2$ (confirmed by ^1H NMR spectroscopy): C, 40.12; H, 3.11; N, 7.20. Found: C, 40.07; H, 2.98; N, 7.10.

[Tp^{Me_2}(PMe$_3$)IrMe(CO)][BAr_f] (3-CO). Method A: A glass vessel sealed to a Kontes vacuum adapter was charged with **3-N_2** (56 mg, 0.038 mmol) and CH_2Cl_2 (3 mL). The solution was degassed and placed under CO (1 atm). The solution was stirred for 24 h, and the solvent was removed under reduced pressure. Crystallization from CH_2Cl_2/pentane afforded **3-CO**. Yield: 43 mg, 77%. **Method B:** A glass vessel sealed to a Kontes vacuum adapter was charged with **10** (40 mg, 0.026 mmol) and CH_2Cl_2 (3 mL). The bright orange solution was heated at 75 °C. After 12 h, the light yellow solution was filtered through glass fiber filter paper and crystallized as described in method A. Yield: 27 mg, 70%. ^1H NMR (400 MHz, CD_2Cl_2, 25 °C): δ 7.72 (bs, 8H, *o*-BAr_f), 7.56 (bs, 4H, *p*-BAr_f), 6.02 (s, 2H, pyrC*H*), 5.88 (s, 1H, pyrC*H*), 2.43 (s, 3H, pyrCH_3), 2.42 (s, 3H, pyrCH_3), 2.40 (s, 3H, pyrCH_3), 2.36 (s, 3H, pyrCH_3), 2.31 (s, 3H, pyrCH_3), 2.30 (s, 3H, pyrCH_3), 1.70 (d, $^2J_{P-H}$ = 11 Hz, 9H, P*Me*$_3$), 1.39 (d, $^3J_{P-H}$ = 3 Hz, 3H, Ir-*Me*). $^{13}C\{^1H\}$ NMR (125 MHz, CD_2Cl_2, 25 °C): δ −22.6 (d, J = 5 Hz, Ir-*C*H$_3$), 13.0 (s, pyr*C*H$_3$), 13.0 (s, pyr*C*H$_3$), 13.4 (s, pyr*C*H$_3$), 14.5 (s, pyr*C*H$_3$), 16.6 (d, $^1J_{P-C}$ = 35 Hz, P*Me*$_3$), 16.7 (s, pyr*C*H$_3$), 17.0 (s, pyr*C*H$_3$), 108.8 (d, $^4J_{P-C}$ = 4 Hz, pyr*C*H), 109.6 (s, pyr*C*H), 111.4 (s, pyr*C*H), 118.1 (septet, $^3J_{F-C}$ = 4 Hz, *p*-BAr_f), 125.2 (q, $^1J_{F-C}$ = 270 Hz, BAr_fCF_3), 129.5 (qq, $^2J_{F-C}$ = 31 Hz, $^4J_{F-C}$ = 3 Hz, *m*-BAr_f), 135.4 (s, *o*-BAr_f), 146.4 (d, J = 3 Hz, pyrC_q), 147.6 (s, pyrC_q), 147.7 (s, pyrC_q), 151.5 (s, J = 3 Hz, pyrC_q), 152.2 (s, pyrC_q), 153.0 (s, pyrC_q), 162.3 (q, $^1J_{B-C}$ = 50 Hz, *i*-BAr_f), 163.3 (d, $^2J_{P-C}$ = 11 Hz, Ir-*C*O). $^{31}P\{^1H\}$ NMR (161.9 MHz, CD_2Cl_2, 25 °C): δ −43.8. ^{19}F (376.5 MHz, CD_2Cl_2, 25 °C): δ −61.0. ^{11}B NMR (160 MHz, CD_2Cl_2, 25 °C): δ −7.2 (BAr_f), −9.5 (d, $^1J_{B-H}$ = 105 Hz, Tp^{Me_2}). IR (KBr): 2965 (w), 2936 (w), 2568 (w, B-H), 2060 (vs, CO), 1610 (m), 1552 (m), 1449 (s), 1422 (s), 1355 (vs), 1278 (vs), 1126 (vs), 960 (m), 888 (m), 839 (m), 793 (w), 745 (w) 713 (w). Anal. Calcd for $C_{52}H_{46}N_6PB_2IrOF_{24}$: C, 42.44; H, 3.15; N, 5.71. Found: C, 42.42; H, 3.16; N, 5.69.

[Tp^{Me_2}(PMe$_3$)IrMe(CH$_3$CN)][BAr_f] (3-CH$_3$CN). To a stirred solution of [Tp^{Me_2}(PMe$_3$)IrMe(N_2)][BAr_f] (30.0 mg, 0.019 mmol) in CH_2Cl_2 (5 mL) was added CH_3CN (1.0 μL, 0.020 mmol). After 1 h, the solution was concentrated, layered with pentane, and cooled to −40 °C. Crystals of **3-CH$_3$CN** were isolated after 3 days. Yield: 26 mg, 83%. ^1H NMR (400 MHz, CD_2Cl_2, 25 °C): δ 7.68 (bs, 8H, *o*-BAr_f), 7.52 (bs, 4H, *p*-BAr_f), 5.92 (s, 1H, pyrC*H*), 5.81 (s, 1H, pyrC*H*), 5.80 (s, 1H, pyrC*H*), 2.63 (s, C*H*$_3$CN), 2.38 (s, 3H, pyrCH_3), 2.37 (s, 3H, pyrCH_3), 2.28 (s, 3H, pyrCH_3), 2.26 (s, 6H, pyrCH_3), 2.25 (s, 3H, pyrCH_3), 1.47 (d, $^2J_{P-H}$ = 10 Hz, 9H, Ir-P*Me*$_3$), 1.46 (d, $^3J_{P-H}$ = 5 Hz, 3H, Ir-*Me*). $^{13}C\{^1H\}$ NMR (125 MHz, CD_2Cl_2): δ −25.6 (d, J = 6 Hz, Ir-*Me*), 12.9 (s, pyr*C*H$_3$), 12.9 (s, pyr*C*H$_3$), 13.7 (s, pyr*C*H$_3$), 13.9 (s, pyr*C*H$_3$), 15.4 (d, $^1J_{P-C}$ = 40 Hz, P*Me*$_3$), 16.2 (s, pyr*C*H$_3$), 16.6 (s, pyr*C*H$_3$), 108.7 (d, $^4J_{P-C}$ = 4 Hz, pyr*C*H), 109.1 (s, pyr*C*H), 110.7 (s, pyr*C*H), 118.1 (septet, $^3J_{F-C}$ = 4 Hz, *p*-BAr_f), 118.9 (s, CH_3CN), 125.2 (q, $^1J_{F-C}$ = 270 Hz, BAr_fCF_3), 129.5 (qq, $^2J_{F-C}$ = 31 Hz, $^4J_{F-C}$ = 3 Hz, *m*-BAr_f), 135.4 (s, *o*-BAr_f), 145.3 (s, pyrC_q), 146.1 (s, pyrC_q), 147.3 (s, pyrC_q), 150.5 (d, $^3J_{P-C}$ = 4 Hz, pyrC_q), 150.8 (s, pyrC_q), 153.8 (s, pyrC_q), 162.4 (q, $^1J_{B-C}$ = 50 Hz, *i*-BAr_f). $^{31}P\{^1H\}$ NMR (161.9 MHz, CD_2Cl_2, 25 °C): δ −49.6. ^{19}F NMR (376.5 MHz, CD_2Cl_2, 25 °C): δ −60.9. ^{11}B NMR (160 MHz, CD_2Cl_2, 25 °C): δ −7.3 (BAr_f), −9.5 (d, $^1J_{B-H}$ = 105 Hz, Tp^{Me_2}). IR (KBr): 2969 (m), 2932 (m), 2561 (m), 2300 (vw), 2237 (vw), 2021 (vw), 1786 (w), 1728 (w), 1611 (m), 1553 (m), 1449 (s), 1421 (s), 1356 (s), 1277 (s), 1144 (vs), 956 (s), 888 (s), 839 (s), 790 (m), 713 (s), 682 (s), 671 (s). FAB/MS (nitrobenzyl alcohol): m/z 622 (M^+), 581 ($M^+ - CH_3CN$). Anal. Calcd for $C_{53}H_{49}N_7PB_2IrF_{24}$: C, 42.87; H, 3.33; N, 6.60. Found: C, 43.21; H, 3.17; N, 6.25.

[Tp^{Me_2}(PMe$_3$)IrMe(AsPh$_3$)][BAr_f] (3-AsPh$_3$). A CH_2Cl_2 (0.5 mL) solution of $AsPh_3$ (7.0 mg, 0.021 mmol) was added to a CH_2Cl_2 (1 mL) solution of [Tp^{Me_2}(PMe$_3$)IrMe(N_2)][BAr_f] (33 mg, 0.021 mmol) kept at −40 °C. After 12 h, the solution was filtered through glass fiber filter paper and the solvent was removed under reduced pressure to yield a light yellow foam. Yield: 38 mg, 100%. This material was determined to be >95% pure by ^1H NMR spectroscopy. Material suitable for combustion analysis was obtained by allowing hexane to diffuse into a concentrated ether solution at 22 °C. Spectroscopic data were obtained on noncrystallized material. ^1H (500 MHz, CD_2Cl_2 25 °C): δ 7.75 (bs, 8H, *o*-BAr_f), 7.60 (bs, 4H, *p*-BAr_f),7.47 (m, 3H, As*Ph*$_3$), 7.38 (bm, 12H, As*Ph*$_3$), 5.86 (s, 2H, pyrC*H*), 5.54 (s, 1H, pyrC*H*), 2.59 (s, 3H, pyr*CH*$_3$), 2.44 (s, 3H, pyr*CH*$_3$), 2.43 (s, 3H, pyr*CH*$_3$), 2.41 (s, 3H, pyr*CH*$_3$), 2.02 (d, $^3J_{P-H}$ = 3 Hz, 3H, Ir*Me*), 1.47 (s, 3H, pyr*CH*$_3$), 1.39 (s, 3H, pyr*CH*$_3$), 1.22 (d, $^2J_{P-H}$ = 10 Hz, 9H, P*Me*$_3$). $^{13}C\{^1H\}$ (125 MHz, CH_2Cl_2, 25 °C): δ −25.3 (s, Ir-*Me*), 13.3 (s, 2 pyr*C*H$_3$), 13.6 (s, pyr*C*H$_3$), 16.1 (s, pyr*C*H$_3$), 16.3 (s, pyr*C*H$_3$), 17.3 (d, $^1J_{P-C}$ = 39 Hz, P*Me*$_3$), 19.3 (s, pyr*C*H$_3$), 109.5 (s, pyr*C*H), 110.3 (d, J_{P-C} = 3 Hz, pyr*C*H), 110.5 (d, J_{P-C} = 5 Hz, pyr*C*H), 118.1 (septet, $^3J_{F-C}$ = 4 Hz, *p*-BAr_f), 125.2 (q, $^1J_{F-C}$ = 270 Hz, BAr_fCF_3), 129.4 (s, As*Ph*$_3$), 129.5 (qq, $^2J_{F-C}$ = 31 Hz, $^4J_{F-C}$ = 3 Hz, *m*-BAr_f), 131.4 (s, As*Ph*$_3$), 132.1 (s, As*Ph*$_3$), 133.2 (s, As*Ph*$_3$), 134.4 (s, As*Ph*$_3$), 135.4 (s, *o*-BAr_f), 146.3 (s, pyrC_q), 147.2 (d, J_{P-C} = 2 Hz, pyrC_q), 147.6 (s, pyrC_q), 151.8 (s, pyrC_q), 153.1 (d, J_{P-C} = 4 Hz, pyrC_q), 162.3 (q, $^1J_{B-C}$ = 50 Hz, *i*-BAr_f). ^{11}B NMR (160 MHz, CD_2Cl_2, 25 °C): δ −7.2 (s, BAr_f), −9.1 (s, Tp^{Me_2}). ^{19}F NMR (376.5 MHz, CD_2Cl_2, 25 °C): δ −60.9. $^{31}P\{^1H\}$ NMR (161.9 MHz, CD_2Cl_2, 25 °C): δ −60.0. IR (KBr): 3072 (w), 2977 (w), 2930 (w), 2565 (w), 1610 (m), 1554 (m), 1441 (m), 1420 (m), 1355 (s), 1280 (s), 1138 (s), 1038 (m), 957 (m), 887 (m), 840 (m), 791 (m), 743 (m), 713 (m). FAB/MS (NBA): m/z 887 (M^+). Anal. Calcd for $C_{69}H_{61}N_6F_{24}PIrB_2\cdot C_6H_{14}$ (confirmed by ^1H NMR spectroscopy): C, 49.06; H, 4.12; N, 4.58. Found: C, 49.31; H, 4.06; N, 4.48.

Tp^{Me_2}(PMe$_3$)IrMe(Cl) (8). An NMR tube was charged with [Tp^{Me_2}(PMe$_3$)IrMe(N_2)][BAr_f] (48 mg, 0.033 mmol) and CH_2Cl_2 (1 mL). The tube was degassed, and PMe_3 (0.033 mmol) was added by vacuum-transfer techniques. After 30 min, the solvent was removed under reduced pressure. The resulting orange foam was dissolved in C_6H_6 (0.5 mL), and over the course of 15 min [Me_3PCH_2Cl][BAr_f] precipitated from solution (spectroscopic and analytical data for [Me_3PCH_2Cl][BAr_f] are listed below). The benzene solution was separated from the precipitate and placed on a plug of silica gel (1 cm × 2 cm). The light yellow band was eluted with CH_2Cl_2. The CH_2Cl_2 was then removed under reduced pressure. This material is contaminated with small amounts (<5%) of [Me_3PCH_2Cl][BAr_f] that we were unable to remove. Yield: 17 mg, 84%. ^1H (500 MHz, CD_2Cl_2 25 °C): δ 5.85 (s, 1H, pyrC*H*), 5.81 (s, 1H, pyrC*H*), 5.77 (s, 1H, pyrC*H*), 2.60 (s, 3H, pyr*CH*$_3$), 2.54 (s, 3H, pyr*CH*$_3$), 2.43 (s, 3H, pyr*CH*$_3$), 2.36 (s, 3H, pyr*CH*$_3$), 2.34 (s, 6H, pyr*CH*$_3$), 1.72 (d, $^3J_{P-H}$ = 4 Hz, 3H, Ir*Me*), 1.50 (d, $^2J_{P-H}$ = 10 Hz, 9H, P*Me*$_3$). $^{13}C\{^1H\}$ (125 MHz, CH_2Cl_2, 25 °C): δ −26.7 (d, $^2J_{P-C}$ = 5 Hz, Ir-*Me*), 13.0 (s, pyr*C*H$_3$), 13.1 (s, pyr*C*H$_3$), 13.7 (s, pyr*C*H$_3$), 14.1 (s, pyr*C*H$_3$), 14.4 (s, pyr*C*H$_3$), 15.5 (d, $^1J_{P-C}$ = 39 Hz, P*Me*$_3$), 16.3 (s, pyr*C*H$_3$), 16.5 (s, pyr*C*H$_3$), 108.4 (d, J_{P-C} = 5 Hz, pyr*C*H), 108.8 (s, pyr*C*H), 109.3 (s, pyr*C*H), 143.6 (d, J = 3 Hz, pyrC_q), 144.5 (s, pyrC_q), 145.3 (s, pyrC_q), 152.0 (d, J_{P-C} = 5 Hz, pyrC_q), 152.5 (s, pyrCq), 152.8

(s, pyrCq). ^{11}B NMR (160 MHz, CD_2Cl_2, 25 °C): δ −9.7 (d, 100 Hz, Tp^{Me_2} *B*-H). $^{31}P\{^1H\}$ NMR (161.9 MHz, CD_2Cl_2, 25 °C): δ −54.5. IR (KBr): 2956 (s), 2918 (s), 2532 (m), 1550 (s), 1442 (s), 1416 (s), 1381 (s), 1271 (s), 1215 (s), 1149 (w), 1115 (m), 1067 (m), 1033 (m), 960 (s), 860 (w), 824 (w), 779 (s), 725 (m), 693 (m), 638 (m), 548 (w), 535 (m). HRMS (EI): *m*/*z* for $[C_{19}H_{34}BClN_6PIr]^+$ (M^+): calcd 616.1994, obsd 616.2008.

[Me$_3$PCH$_2$Cl][BAr$_f$]. See the synthesis of $Tp^{Me_2}(PMe_3)IrMe(Cl)$ (**8**) described above for preparative procedure. Yield: 19 mg, 58%. ^{1}H (500 MHz, CD_2Cl_2 25 °C): δ 7.74 (bs, 8H, *o*-BAr$_f$), 7.60 (bs, 4H, *p*-BAr$_f$), 3.99 (d, $^2J_{P-H}$ = 6 Hz, 2H, ClC*H*$_2$PMe$_3$), 2.00 (d, $^2J_{P-H}$ = 14 Hz, 9H, ClCH$_2$P*Me*$_3$). $^{13}C\{^1H\}$ (125 MHz, CH_2Cl_2, 25 °C): δ 7.9 (d, $^1J_{P-C}$ = 55 Hz, ClCH$_2$P*Me*$_3$), 33.3 (d, $^1J_{P-C}$ = 55 Hz, Cl*C*H$_2$PMe$_3$), 118.1 (septet, $^3J_{F-C}$ = 4 Hz, *p*-BAr$_f$), 125.2 (q, $^1J_{F-C}$ = 270 Hz, BAr$_f$*C*F$_3$), 129.5 (qq, $^2J_{F-C}$ = 31 Hz, $^4J_{F-C}$ = 3 Hz, *m*-BAr$_f$), 135.4 (s, *o*-BAr$_f$), (q, $^1J_{B-C}$ = 50 Hz, *i*-BAr$_f$). ^{11}B NMR (160 MHz, CD_2Cl_2, 25 °C): δ −7.3 (s, BAr$_f$). ^{19}F NMR (376.5 MHz, CD_2Cl_2, 25 °C): δ −60.8. $^{31}P\{^1H\}$ NMR (161.9 MHz, CD_2Cl_2, 25 °C): δ 30.9. IR (KBr): 3095 (w), 3013 (w), 2934 (w), 1788 (m), 1611 (m), 1426 (m), 1357 (s), 1278 (s), 1130 (s), 961 (m), 887 (m), 838 (m), 710 (m), 671 (m). HRMS (FAB/NBA) *m*/*z* for $[C_4H_{11}PCl]^+$ (M^+): calcd 125.0287, obsd 125.0284. Anal. Calcd for $C_{36}H_{23}BClPF_{24}$: C, 43.73; H, 2.34. Found: C, 43.99; H, 2.12.

[Tp^{Me_2}(PMe$_3$)Ir(N$_2$)(Ph)][BAr$_f$] (9). To a solution of **3-N$_2$** (35 mg, 0.023 mmol) in CH_2Cl_2 (3 mL) was added a solution of C_6H_6 (2 μl, 0.023 mmol) in CH_2Cl_2 (1 mL). After 15 h at room temperature, the solution was filtered and the solvent was removed under reduced pressure. Yield: 28 mg, 76%. This material was ∼90% pure as determined by ^{1}H NMR spectroscopy. Material suitable for single-crystal X-ray analysis was obtained by slow diffusion of pentane into a concentrated solution of $[Tp^{Me_2}(PMe_3)IrPh(N_2)][BAr_f]$ in CH_2Cl_2 at −40 °C. ^{1}H NMR (400 MHz, CD_2Cl_2, 25 °C): δ 7.69 (bs, 8H, *o*-BAr$_f$), 7.52 (bs, 4H, *p*-BAr$_f$), 7.24 (d, ^{1}H, J_{H-H} = 7 Hz, C_6H_5), 7.15 (t, ^{1}H, J_{H-H} = 7 Hz, C_6H_5), 7.07 (t, ^{1}H, J_{H-H} = 7 Hz, C_6H_5), 6.86 (t, ^{1}H, J_{H-H} = 8 Hz, C_6H_5), 6.23 (d, ^{1}H, J_{H-H} = 8 Hz, C_6H_5), 6.01 (s, 1H, pyrC*H*), 5.92 (s, 1H, pyrC*H*), 5.80 (s, 1H, pyrC*H*), 2.45 (s, 3H, pyrCH_3), 2.43 (s, 3H, pyrCH_3), 2.40 (s, 3H, pyrCH_3), 2.34 (s, 3H, pyrCH_3), 1.60 (d, 9H, $^2J_{P-H}$ = 10 Hz, Ir-P*Me*$_3$), 1.58 (s, 3H, pyrCH_3), 1.38 (s, 3H, pyrCH_3). $^{13}C\{^1H\}$ NMR (125 MHz, CD_2Cl_2): δ 12.9 (s, pyr*C*H$_3$), 13.6 (s, pyr*C*H$_3$), 13.8 (s, pyr*C*H$_3$), 16.2 (d, $^1J_{P-C}$ = 40 Hz, P*Me*$_3$), 16.4 (s, pyr*C*H$_3$), 18.7 (s, pyr*C*H$_3$), 109.3 (d, $^4J_{P-C}$ = 4 Hz, pyr*C*H), 110.1 (s, pyr*C*H), 111.2 (s, pyr*C*H), 118.1 (septet, $^3J_{F-C}$ = 4 Hz, *p*-BAr$_f$), 125.2 (q, $^1J_{F-C}$ = 270 Hz, BAr$_f$*C*F$_3$), 126.2 (s, *C*$_6$H$_5$), 128.9 (s, *C*$_6$H$_5$), 128.8 (s, *C*$_6$H$_5$), 129.5 (qq, $^2J_{F-C}$ = 31 Hz, $^4J_{F-C}$ = 3 Hz, *m*-BAr$_f$), 135.4 (s, *o*-BAr$_f$), 140.0 (s, *C*$_6$H$_5$), 138.0 (d, $^3J_{P-C}$ = 5 Hz, *C*$_6$H$_5$), 142.2 (d, $^2J_{P-C}$ = 9 Hz, *C*$_6$H$_5$), 146.0 (d, $^3J_{P-C}$ = 4 Hz, pyr*C*$_q$), 147.3 (s, pyr*C*$_q$), 148.3 (s, pyr*C*$_q$), 151.7 (s, pyr*C*$_q$), 151.8 (d, $^3J_{P-C}$ = 4 Hz, pyr*C*$_q$), 153.6 (d, $^5J_{P-C}$ = 1 Hz, pyr*C*$_q$), 162.4 (q, $^1J_{B-C}$ = 50 Hz, *i*-BAr$_f$). $^{31}P\{^1H\}$ NMR (161.9 MHz, CD_2Cl_2, 25 °C): δ −48.9. ^{19}F NMR (376.5 MHz, CD_2Cl_2, 25 °C): δ −61.0. ^{11}B NMR (160 MHz, CD_2Cl_2, 25 °C): δ −7.3 (BAr$_f$), −9.5 (d, $^1J_{B-H}$ = 102 Hz, Tp^{Me_2}). IR (KBr): 3055 (w), 2970 (w), 2929 (w), 2567 (m), 2236 (s), 1611 (m), 1551 (s), 1449 (s), 1421 (s), 1356 (s), 1278 (s), 1162 (s), 1073 (s), 959 (m), 888 (m), 839 (m), 794 (w), 713 (m), 682 (m), 671 (m). HRMS (FAB, nitrobenzyl alcohol): *m*/*z* for $[C_{24}H_{36}BN_6PIr]^+$ ($M^+ - N_2$): calcd 643.2497, obsd 643.2461.

[Tp^{Me_2}(PMe$_3$)IrMe(HC(O)CH$_3$)][BAr$_f$] (10). A glass vessel sealed to a Kontes vacuum adapter was charged with **3-N$_2$** (64 mg, 0.043 mmol), a stir bar, and CH_2Cl_2 (2 mL). The solution was degassed, and acetaldehyde (0.047 mmol) was added via vacuum-transfer techniques. After stirring the solution at 22 °C for 12 h, the reaction vessel was brought into a glovebox. The solution was transferred to a 20 mL vial, concentrated to ∼0.5 mL in vacuo, layered with pentane, and cooled to −40 °C. Light-yellow crystals of $[Tp^{Me_2}(PMe_3)IrMe(HC(O)CH_3)][BAr_f]$ were isolated and rinsed with cold pentane. Yield: 40 mg, 60%. ^{1}H NMR (400 MHz, CD_2Cl_2, 25 °C): δ 9.23 (q, 1H, $^3J_{H-H}$ = 4 Hz, $CH_3C(O)H$), 7.73 (bs, 8H, *o*-BAr$_f$), 7.57 (bs, 4H, *p*-BAr$_f$), 5.96 (s, 1H, pyrC*H*), 5.85 (s, 1H, pyrC*H*), 5.79 (s, 1H, pyrC*H*), 2.43 (s, 3H, pyrCH_3), 2.43 (s, 3H, pyrCH_3), 2.41 (d, 3H, $^3J_{H-H}$ = 4 Hz, CH_3C(O)H), 2.32 (s, 6H, pyrCH_3), 1.97 (s, 3H, pyrCH_3), 1.94 (s, 3H, pyrCH_3), 1.78 (d, 3H, $^3J_{P-H}$ = 2 Hz, Ir-*Me*), 1.48 (d, 9H, $^2J_{P-H}$ = 10 Hz, P*Me*$_3$). $^{13}C\{^1H\}$ NMR (125 MHz, CD_2Cl_2, 25 °C): δ 223.7 (s, $CH_3C(O)H$), 162.4 (q, $^1J_{B-C}$ = 50 Hz, *i*-BAr$_f$), 155.2 (s, pyr*C*$_q$), 149.1 (d, $^3J_{P-C}$ = 4 Hz, pyr*C*$_q$), 148.8 (s, pyr*C*$_q$), 148.0 (s, pyr*C*$_q$), 146.3 (s, pyr*C*$_q$), 145.9 (d, $^5J_{P-C}$ = 2 Hz, pyr*C*$_q$), 135.4 (s, *o*-BAr$_f$), 129.5 (qq, $^2J_{F-C}$ = 31 Hz, $^4J_{F-C}$ = 3 Hz, *m*-BAr$_f$), 125.2 (q, $^1J_{F-C}$ = 270 Hz, BAr$_f$*C*F$_3$), 118.1 (septet, $^3J_{F-C}$ = 4 Hz, *p*-BAr$_f$), 110.7 (s, pyr*C*H), 109.3 (s, pyr*C*H), 109.2 (d, $^4J_{P-C}$ = 4 Hz, pyr*C*H), 32.2 (s, *C*H$_3$C(O)H), 16.4 (s, pyr*C*H$_3$), 15.7 (s, pyr*C*H$_3$), 14.9 (d, $^1J_{P-C}$ = 40 Hz, P*Me*$_3$), 13.8 (s, pyr*C*H$_3$), 13.7 (s, pyr*C*H$_3$), 12.9 (s, pyr*C*H$_3$), 12.8 (s, pyr*C*H$_3$), −24.8 (d, J = 6 Hz, Ir-*Me*). $^{31}P\{^1H\}$ NMR (161.9 MHz, CD_2Cl_2, 25 °C): δ −43.8. ^{19}F NMR (376.5 MHz, CD_2Cl_2, 25 °C): δ −60.9.^{11}B NMR (160 MHz, CD_2Cl_2, 25 °C): δ −7.2 (BAr$_f$), 9.5 (d, $^1J_{B-H}$ = 108 Hz). IR (KBr): 2935 (w), 2560 (w), 1650 (m), 1610 (m), 1550 (m), 1447 (m), 1421 (m), 1355 (s), 1278 (s), 1278 (s), 1163 (s), 1073 (w), 950 (m), 890 (m), 849 (m), 792 (w), 714 (m), 683 (m), 671 (m). Anal. Calcd for $C_{53}H_{50}N_6PB_2IrOF_{24}\cdot 1/2CH_2Cl_2$ (confirmed by ^{1}H NMR spectroscopy): C, 41.99; H, 3.36; N, 5.49. Found: C, 42.26; H, 3.28; N, 5.31.

[Tp^{Me_2}(PMe$_3$)IrMe(HC(O)C$_6$H$_4$CH$_3$)][BAr$_f$] (11). To a vial containing a solution of $[Tp^{Me_2}(PMe_3)IrMe(N_2)][BAr_f]$ (40.2 mg, 0.028 mmol) in CH_2Cl_2 (3 mL) was added *p*-tolualdehyde (3.3 μL, 0.028 mmol) via syringe. Upon addition the solution turned bright orange. The solvent was removed under reduced pressure after 30 min at 22 °C to yield a bright yellow solid. The product was dissolved in a minimum of CH_2Cl_2, layered with pentane, and cooled to −40 °C. Over the course of 5 days, yellow needlelike crystals of **11** formed. Yield: 38 mg, 87%. ^{1}H NMR (500 MHz, CD_2Cl_2, 25 °C): δ 1.55 (d, 9H, $^2J_{P-H}$ = 10 Hz, P*Me*$_3$), 1.86 (d, 3H, $^3J_{P-H}$ = 4 Hz, Ir-*Me*), 1.90 (s, 3H, pyrCH_3), 1.91 (s, 3H, pyrCH_3), 2.39 (s, 6H, pyrCH_3), 2.47 (s, 3H, HC(O)C$_6$H$_4$CH_3), 2.48 (s, 3H, pyrCH_3), 2.54 (s, 3H, pyrCH_3), 5.85 (s, 1H, pyrC*H*), 5.86 (s, 1H, pyrC*H*), 5.98 (s, 1H, pyrC*H*), 7.42 (d, $^3J_{H-H}$ = 8 Hz, HC(O)C$_6$*H*$_4$CH$_3$), 7.58 (bs, 4H, *p*-BAr$_f$), 7.58 (d, HC(O)C$_6$H$_4$CH$_3$, obscured by BAr$_f$ resonance), 7.75 (bs, 8H, *o*-BAr$_f$), 9.18 (s, *H*C(O)C$_6$H$_4$CH$_3$). $^{13}C\{^1H\}$ NMR (125 MHz, CD_2Cl_2, 25 °C): δ −24.6 (d, $^2J_{P-C}$ = 8 Hz, Ir-*Me*), 12.9 (s, pyr*C*H$_3$), 13.0 (s, pyr*C*H$_3$), 13.7 (s, pyr*C*H$_3$), 13.9 (s, pyr*C*H$_3$), 15.0 (d, $^1J_{P-C}$ = 39 Hz, P*Me*$_3$), 15.8 (s, pyr*C*H$_3$), 16.4 (s, pyr*C*H$_3$), 22.9 (s, HC(O)C$_6$H$_4$*C*H$_3$), 109.1 (d, $^3J_{P-C}$ = 4 Hz, pyr*C*H), 109.2 (s, pyr*C*H), 110.5 (s, pyr*C*H), 118.1 (septet, $^3J_{F-C}$ = 4 Hz, *p*-BAr$_f$), 125.2 (q, $^1J_{F-C}$ = 270 Hz, BAr$_f$*C*F$_3$), 129.5 (qq, $^2J_{F-C}$ = 31 Hz, $^4J_{F-C}$ = 3 Hz, *m*-BAr$_f$), 131.6 (s, HC(O)*C*$_6$H$_4$CH$_3$), 132.3 (s, *p*-HC(O)*C*$_6$H$_4$CH$_3$), 135.4 (s, *o*-BAr$_f$), 145.7 (d, J = 3 Hz, pyr*C*$_q$), 146.2 (s, pyr*C*$_q$), 147.8 (s, *i*-HC(O)*C*$_6$H$_4$CH$_3$), 149.1 (s, pyr*C*$_q$), 149.4 (s, pyr*C*$_q$), 153.0 (s, pyr*C*$_q$), 155.1 (s, pyr*C*$_q$), 162.3 (q, $^1J_{B-C}$ = 50 Hz, *i*-BAr$_f$), 207.6 (s, H*C*(O)*C*$_6$H$_4$CH$_3$). $^{31}P\{^1H\}$ NMR (161.9 MHz, CD_2Cl_2, 25 °C): δ −46.6. ^{19}F NMR (376.5 MHz, CD_2Cl_2, 25 °C): δ −61.0.^{11}B NMR (160 MHz, CD_2Cl_2, 25 °C): δ −7.3 (s, BAr$_f$), 9.6 (s, Tp^{Me_2}). IR (KBr): 2973 (m), 2935(m), 2562 (w, B−H), 1610 (m), 1592 (s), 1562 (m), 1355 (s), 1278 (s), 1127 (s), 958 (m), 888 (m), 840 (m), 713 (m), 681 (m), 671 (m). FAB/MS (sulfolane): *m*/*z* 701 (M^+). Anal. Calcd for $C_{59}H_{54}N_6PB_2IrOF_{24}$: C, 45.31; H, 3.48; N, 5.36. Found: C, 44.90; H, 3.62; N, 5.00.

[Tp^{Me_2}(PMe$_3$)Ir(C$_6$H$_4$CH$_3$)(CO)][BAr$_f$] (12). A glass vessel sealed to a Kontes vacuum adapter was charged with $[Tp^{Me_2}(PMe_3)IrMe(N_2)][BAr_f]$ (43 mg, 0.027 mmol), *p*-tolualdehyde (9.7 μL, 0.082 mmol), and CH_2Cl_2 (10 mL). The bright orange solution was heated at 105 °C. After 36 h, the solution had turned light yellow; it was filtered through glass fiber filter paper, concentrated, layered with pentane, and cooled to −40 °C. Colorless crystals of **12** were isolated and washed with a cold solution of pentane/CH_2Cl_2. Yield: 37 mg, 83%. The pentane molecule of crystallization is not reported in the

spectroscopic data. ^{1}H NMR (500 MHz, CD_2Cl_2, 25 °C): δ 7.75 (bs, 8H, *o*-BAr_f), 7.60 (bs, 4H, *p*-BAr_f), 7.30 (d, 1H, J_{H-H} = 8 Hz, $C_6H_4CH_3$), 7.00 (d, 1H, J_{H-H} = 6 Hz, $C_6H_4CH_3$), 6.75 (d, 1H, J_{H-H} = 7 Hz, $C_6H_4CH_3$), 6.20 (d, 1H, J_{H-H} = 7 Hz, C_6H_4-CH_3), 6.06 (s, 1H, pyrC*H*), 6.03 (s, 1H, pyrC*H*), 5.85 (s, 1H, pyrC*H*), 2.50 (s, 3H, C_6H_4CH3), 2.47 (s, 3H, pyrCH_3), 2.44 (s, 3H, pyrCH_3), 2.38 (s, 3H, pyrCH_3), 2.37 (s, 3H, pyrCH_3), 2.31 (s, 3H, pyrCH_3), 1.72 (d, 9H, $^2J_{P-H}$ = 9 Hz, P*Me*$_3$), 1.69 (s, 3H, pyrCH_3), 1.53 (s, 3H, pyrCH_3). ^{13}C{^{1}H} NMR (125 MHz, CD_2-Cl_2, 25 °C): δ 13.0 (s, pyr*C*H$_3$), 13.0 (s, pyr*C*H$_3$), 13.5 (s, $C_6H_4CH_3$), 14.3 (s, pyr*C*H$_3$), 16.9 (s, pyr*C*H$_3$), 17.2 (d, $^1J_{P-C}$ = 41 Hz, P*Me*$_3$), 18.3 (s, pyr*C*H$_3$), 20.9 (s, pyr*C*H$_3$), 109.0 (d, $^3J_{P-C}$ = 4 Hz, pyr*C*H), 109.8 (s, pyr*C*H), 111.1 (s, pyr*C*H), 115.9 (d, $^2J_{P-C}$ = 8 Hz, $C_6H_4CH_3$), 118.1 (septet, $^3J_{F-C}$ = 4 Hz, *p*-BAr_f), 125.2 (q, $^1J_{F-C}$ = 270 Hz, BAr_fCF_3), 129.5 (qq, $^2J_{F-C}$ = 31 Hz, $^4J_{F-C}$ = 3 Hz, *m*-BAr_f), 130.1 (s, $C_6H_4CH_3$), 130.5 (s, $C_6H_4CH_3$), 135.4 (s, *o*-BAr_f), 136.2 (s, $C_6H_4CH_3$), 139.0 (s, $C_6H_4CH_3$), 140.1 (d, $^3J_{P-C}$ = 5 Hz, $C_6H_4CH_3$), 146.5 (d, $^3J_{P-C}$ = 3 Hz, pyrC_q), 147.7 (s, pyrC_q), 148.0 (s, pyrC_q), 152.0 (d, $^3J_{P-C}$ = 3 Hz, pyrC_q), 153.5 (s, pyrC_q), 162.3 (q, $^1J_{B-C}$ = 50 Hz, *i*-BAr_f), 162.9 (d, $^2J_{P-C}$ = 11 Hz, Ir-*C*O). ^{31}P{^{1}H} NMR (161.9 MHz, CD_2Cl_2, 25 °C): δ −45.3. ^{19}F NMR (376.5 MHz, CD_2Cl_2, 25 °C): δ −61.0. ^{11}B NMR (160 MHz, CD_2Cl_2, 25 °C): δ −7.3 (s, BAr_f), −9.3 (s, Tp^{Me_2}). IR (KBr): 2967 (w), 2930 (w), 2570 (w), 2069 (s), 1611 (m), 1551 (m), 1450 (m), 1422 (m), 1355 (s), 1280 (s), 1129 (s), 1074 (m), 960 (m), 888 (m), 805 (w), 745 (w), 714 (m), 682 (m), 671 (m). FAB/MS (NBA): *m*/*z* 685 (M^+). Anal. Calcd for $C_{53}H_{40}N_6PB_2IrOF_{24}$·$CH_3(CH_2)_3CH_3$·$CH_2Cl_2$ (confirmed by ^{1}H NMR spectroscopy): C, 45.09; H, 3.78; N, 4.93. Found: C, 44.91; H, 3.63; N, 5.20.

[Tp^{Me_2}(PMe$_3$)IrH(N$_2$)][BAr_f] (13). A glass vessel (100 mL) sealed to a Kontes vacuum adapter was charged with [Tp^{Me_2}-(PMe$_3$)Ir(C(N$_2$)][BAr_f] (95 mg, 0.061 mmol), CH_2Cl_2 (10 mL), and a stirbar. The solution was freeze−pump−thaw degassed (3×), placed under H_2 (1 atm), and allowed to stir. After 1.5 h, the solvent was removed under reduced pressure to yield an off-white solid. ^{1}H NMR spectroscopic analysis (CD_2Cl_2) of the solid revealed a 1:1 mixture of the desired product and [Tp^{Me_2}-(PMe$_3$)IrH(H$_2$)][BAr_f]. The powder was redissolved in CH_2Cl_2 (20 mL) and transferred to a Parr Bomb containing a stirbar. The bomb was pressurized with N_2 (40 atm), and the solution was allowed to stir. After 12 h, the bomb was vented and repressurized with N_2 (40 atm). After an additional 12 h, the bomb was vented, and the solvent was removed under reduced pressure to yield [Tp^{Me_2}(PMe$_3$)IrH(N$_2$)][BAr_f]. White microcrystals of **13** are obtained after crystallization from CH_2Cl_2/pentane at −40 °C. Yield: 60 mg, 64%. ^{1}H (500 MHz, CD_2Cl_2 25 °C): δ 7.70 (bs, 8H, *o*-BAr_f), 7.60 (bs, 4H, *p*-BAr_f), 6.07 (s, 1H, pyrC*H*), 5.98 (s, 1H, pyrC*H*), 5.85 (s, 1H, pyrC*H*), 2.49 (s, 3H, pyrCH_3), 2.43 (s, 3H, pyrCH_3), 2.40 (s, 3H, pyrCH_3), 2.29 (s, 3H, pyrCH_3), 2.27 (s, 6H, pyrCH_3), 1.65 d, $^2J_{P-H}$ = 11 Hz, 9H, P*Me*$_3$), −18.80 (d, $^2J_{P-H}$ = 19 Hz, 1H, P*Me*$_3$). ^{13}C{^{1}H} (125 MHz, CH_2Cl_2, 25 °C): δ 12.7 (s, pyr*C*H$_3$), 12.8 (s, pyr*C*H$_3$), 13.4 (s, pyr*C*H$_3$), 14.9 (s, pyr*C*H$_3$), 15.8 (s, pyr*C*H$_3$), 17.5 (d, $^1J_{P-C}$ = 41 Hz, P*Me*$_3$), 18.0 (s, pyr*C*H$_3$), 107.0 (d, $^3J_{P-C}$ = 3 Hz, pyr*C*H), 109.2 (s, pyr*C*H), 109.3 (s, pyr*C*H), 118.1 (septet, $^3J_{F-C}$ = 4 Hz, *p*-BAr_f), 125.2 (q, $^1J_{F-C}$ = 270 Hz, BAr_fCF_3), 129.5 (qq, $^2J_{F-C}$ = 31 Hz, $^4J_{F-C}$ = 3 Hz, *m*-BAr_f), 135.4 (s, *o*-BAr_f), 146.5 (d, *J* = 3 Hz, pyrC_q), 147.1 (s, pyrC_q), 149.5 (s, pyrC_q), 151.0 (d, *J* = 3 Hz, pyrC_q), 151.9 (s, pyrC_q), 154.1 (s, pyrC_q), 162.3 (q, $^1J_{B-C}$ = 50 Hz, *i*-BAr_f). ^{11}B NMR (160 MHz, CD_2Cl_2, 25 °C): δ −7.3 (s, BAr_f), −9.1 (d, $^1J_{B-H}$ = 96 Hz, Tp^{Me_2}). ^{19}F NMR (376.5 MHz, CD_2Cl_2, 25 °C): δ −61.0. ^{31}P{^{1}H} NMR (161.9 MHz, CD_2Cl_2, 25 °C): δ −46.7. IR (KBr): 2968 (w), 2925 (w), 2562 (w, B-H), 2231 (m, N_2), 2205 (w, Ir-H), 1610.5 (m), 1550 (m), 1449 (m), 1423 (m), 1386 (m), 1355 (s), 1279 (s), 1129 (s), 960 (s), 839 (w), 796 (w), 714 (w), 671 (w). Anal. Calcd for $C_{50}H_{44}N_8F_{24}PIrB_2$: C, 41.20; H, 3.04; N, 7.69. Found: C, 40.85; H, 2.83; N, 7.38.

Spectroscopic Observation of [Cp*(PMe$_3$)IrMe(N$_2$)]-[BAr_f] (2-N$_2$). NMR Spectroscopy. A CD_2Cl_2 (0.2 mL) solution of [Cp*(PMe$_3$)IrMe(CH_2Cl_2)][BAr_f] (15 mg, 0.011 mmol) was transferred to an NMR tube equipped with a 1/4 in. male Teflon cap. The tube was attached through the cap to a nitrogen manifold fitted with a gauge, and the solution was placed under N_2 (8 atm). The tube was then removed from the apparatus and shaken for ∼1 min. *Caution: The tube was agitated using a mechanical stirrer which was kept behind a blast shield.* ^{1}H and ^{31}P{^{1}H} NMR spectra were then acquired. ^{1}H NMR (500 MHz, CD_2Cl_2, 25 °C): δ 7.74 (bs, 8H, *o*-BAr_f), 7.50 (bs, 4H, *p*-BAr_f), 1.68 (d, $^4J_{P-H}$ = 1 Hz, 15H, C_5Me_5, this differed by 0.02 ppm from **2-CH_2Cl_2**), 1.57 (d, $^2J_{P-H}$ = 17 Hz, 9H, P*Me*$_3$, this differed by 0.002 ppm from **2-CH_2Cl_2**), 1.18 (d, $^3J_{P-H}$ = 6 Hz, 3H, Ir-*Me*, this differed by −0.064 ppm from **2-CH_2Cl_2**). ^{31}P{^{1}H} NMR (202.4 MHz, CD_2Cl_2, 25 °C): δ −27.9 (this differed by 1.20 ppm from **2-CH_2Cl_2**). **IR Spectroscopy**: In a glovebox, a CH_2Cl_2 (5 mg) solution of [Cp*(PMe$_3$)IrMe(CH_2-Cl_2)][BAr_f] (30.1 mg, 0.053 mmol) was transferred to a high-pressure infrared cell.[100] The cell was sealed, removed from the box, and pressurized with nitrogen. IR(CH_2Cl_2): 2207 (N_2).

X-ray Structure Determinations. The X-ray diffraction measurements were made on a Siemens SMART diffractometer[101] with a CCD area detector. The crystal was mounted on a glass fiber using Paratone N hydrocarbon oil. Cell constants and an orientation matrix for data collection were obtained from a least-squares refinement using the measured positions of reflections in the range 3.00° < 2θ < 45.00°. Data were integrated using the program SAINT.[102] No decay correction was applied. An empirical absorption correction based on comparison of redundant and equivalent data and an ellipsoidal model of the absorption surface was applied using the program XPREP[103] or SADABS (**7**: T_{max} = 0.69, T_{min} = 0.0.56; **3-N$_2$**: T_{max} = 0.80, T_{min} = 0.46; **9**: T_{max} = 0.74, T_{min} = 0.64).[104] The structures were solved using methods described previously.[105] The function minimized in the full-matrix least-squares refinement was $\sum w(|F_o| - |F_c|)^2$. The weighting scheme was based on counting statistics and included a factor to downweight the intense reflections. Positional and thermal parameters for the non-hydrogen atoms and the complete list of intramolecular distances and angles for the complexes are given in the Supporting Information.

(a) [Tp^{Me_2}(PMe$_3$)IrMe(N$_2$)][BAr_f] (3-N$_2$). The compound crystallizes in the space group *C*2/*c* (no. 15) with eight formula units in the unit cell. The methyl and dinitrogen ligands are disordered over the two coordination sites in a 47:53 ratio. The dinitrogen was assumed to be linearly coordinated, and the methyl group was assumed to lie on the same vector as dinitrogen. Due to the close proximity of the atoms involved in the disorder, the positions of only the terminal nitrogen atoms of the N_2 ligand (N7 and N8) were refined. The fluorine atoms of some of the CF_3 groups on the BAr_f anion were disordered. The occupancies of the disordered fluorine atoms in the BAr_f anion were adjusted so that the isotropic thermal parameters of the disordered components were roughly equal; the sum of the occupancies of the fluorine atoms of each CF_3 group was equal to three. The non-hydrogen atoms (except for the boron atoms and the partial occupancy chlorine, carbon, fluorine, and nitrogen atoms) were refined anisotropically. The

(99) Brookhart, M.; Grant, B.; Volpe, A. F. *Organometallics* **1992**, *11*, 3920−3922.
(100) Schultz, R. H.; Bengali, A. A.; Tauber, M. J.; Weiller, B. H.; Wasserman, E. P.; Kyle, K. R.; Moore, C. B.; Bergman, R. G. *J. Am. Chem. Soc.* **1994**, *116*, 7369−7377.
(101) *SMART Area-Detector Software Package*; Siemens Industrial Automation, Inc.: Madison, WI, 1995.
(102) *SAINT: SAX Area-Detector Integration Program*, V4.024; Siemens Industrial Automation, Inc.: Madison, WI, 1995.
(103) *XPREP (v 5.03)*, Part of the SHELXTL Crystal Structure Determination Package; Siemens Industrial Automation, Inc.: Madison, WI, 1995.
(104) Sheldrick, G. *SADABS Siemens Area Detector ABSorption correction program*; 1996. Advance copy, private communication.
(105) Kaplan, A. W.; Polse, J. L.; Ball, G. E.; Andersen, R. A.; Bergman, R. G. *J. Am. Chem. Soc.* **1998**, *120*, 11649−11662.

partial occupancy fluorine atoms, the terminal N atoms of the disordered dinitrogen ligand (N7, N8), and the partial occupancy carbon (C53) and chlorine atoms (Cl3, Cl5) of the disordered CH_2Cl_2 molecules were refined isotropically.

(b) $Tp^{Me_2}(PMe_3)IrMe(OTf)$ (7). The compound crystallizes in the space group $P2_1/c$ (no. 14) with four formula units in the unit cell. The non-hydrogen atoms, except for Cl(2) and C(21) of the disordered solvent, were refined anisotropically. The hydrogen atoms, Cl(2), and C(21) were refined isotropically.

(c) $[Tp^{Me_2}(PMe_3)IrPh(N_2)][BAr_f]$ (9). The compound crystallizes in the space group $P2_1/C$ (no. 14) with four molecules in the unit cell. The asymmetric unit consists of the iridium complex cation, a BAr_f anion, and a pentane of crystallization. The non-hydrogen atoms (except the partial occupancy carbon and fluorine atoms) were refined anisotropically. The partial occupancy fluorine atoms (F(1)−F(3) and F(22)−F(36)) and carbon atoms (C(58) and C(60)−C(65)) were refined isotropically. Two of the CF_3 groups on the BAr_f anion show a three-part rotational disorder, modeled with a 40:40:20% occupancy ratio. Inspection of the Fourier map clearly shows that this is a lightly hindered rotation of the CF_3 groups. The pentane of crystallization shows considerable disorder. The two terminal carbons (C57 and C59) were refined with full occupancy and anisotropic thermal motion parameters. The remaining carbon atoms were modeled with isotropic thermal parameters constrained to be equal, and their occupancies were allowed to refine.

Acknowledgment. This work was supported by the Director, Office of Energy Research, Office of Basic Energy Sciences, Chemical Sciences Division, U.S. Department of Energy, under Contract No. DE-AC03-76SF00098. The Center for New Directions in Organic Synthesis is supported by Bristol-Myers Squibb as Sponsoring Member. We thank Dr. Fred Hollander and Dr. Dana Caulder of the UC Berkeley CHEXRAY facility for the X-ray structure determinations, Professors D. M. Heinekey and Ernesto Carmona for helpful discussions, and Dr. Jake Yeston and Dr. Jeffrey T. Golden for assistance with high-pressure N_2 experiments. We also thank Boehringer-Ingelheim Pharmaceuticals, Inc. for a graduate fellowship to D.M.T.

Supporting Information Available: ORTEP diagrams and tables of atomic coordinates, anisotropic displacement parameters, bond lengths and bond angles for compounds **3-N_2**, **7**, and **9**. These materials are available free of charge via the Internet at http://pubs.acs.org.

OM010697C